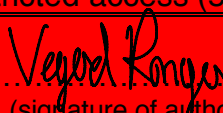




Universitetet
i Stavanger

FACULTY OF SCIENCE AND TECHNOLOGY

MASTER THESIS

Study programme/specialisation: Industrial Economics	Spring semester, 2018 Restricted access (5 years)
Author: Vegard Gloppholm Rongve	 (signature of author)
Faculty supervisor: Helge Hodne	
External supervisors: Arne G. Larsen (HydraWell Intervention) Morten Myhre (HydraWell Intervention)	
Title of master thesis: Optimize the HydraArchimedes™ cement insurance tool	
Credits : 30	
Keywords: Plug & Abandonment Cement Insurance Tool HydraArchimedes™ 3D-printer Impeller RPM Pressure generation Dye Computational Fluid Dynamics	Number of pages: 65 +supplemental material/other: 1 Stavanger, 09.06.18 Date, year

Acknowledgement

This thesis is submitted as part of my Master of Science (M.Sc.) program at the University of Stavanger (UiS). It would not have been possible to complete this work without support, guidance, and help for many individuals. Therefore, I would like to use this opportunity to express my gratitude towards all of them.

Firstly, I would like to thank my supervisor at the University of Stavanger, Helge Hodne for giving me valuable and structured feedback and assistance during the process of writing my thesis. His willingness to give his time so generously has been very much appreciated.

Secondly, I would like to state my largest gratitude to HydraWell Intervention and their employees for supporting me with valuable information and technical support. A special message of gratitude goes to Morten Myhre and Arne G. Larsen for excellent guidance, encouragement and feedback. In spite of being very busy in their positions, they have always taken time for me. Without their technical insight and experience this thesis would not be the same.

Finally, I would like to thank my family and friends for all the help and support during my studies.

Abstract

The HydraArchimedes™ tool is called a cement insurance tool because of its ability to squeeze cement out through casing perforations by rotating the tool inside a casing, thereby creating a rock-to-rock barrier. It is therefore essential that the design of the tool is optimal to allow the tool to properly fill the annular space behind the casing with cement during a plug and abandonment (P&A) operation, thereby preventing oil and gas from migrating to the surface through holes and/or cracks in the cement plug.

This Master's thesis builds on the Bachelor's thesis called "Build and optimize a test-rig that can simulate the differential pressure produced by the HydraArchimedes™ during a P&A operation, as a function of angular velocity", which was written by Vegard Rongve and Tor Kristian Opaas for HydraWell Intervention in 2016. The main purpose of the Bachelor's thesis was to design and build a test-rig that could simulate a small-scale version of the situation in the well and also to analyze the pressure generated by the HydraArchimedes™ cement insurance tool during the operation. In the present Master's thesis, the objective was to modify the test-rig and to examine different cement insurance tool designs in order to optimize HydraWell's perforate-wash-cement technology (PWC®). A 3D-printer was used to manufacture alternative plastic prototypes, and a pressure transmitter was used to record the pressure. Water containing dye and a computational fluid dynamics (CFD) analysis were then used to analyze the tool's displacement effect on the water on the outside of the casing.

The results of this Master's thesis indicate that the cement displacement efficiency of the current HydraArchimedes™ design can be increased. It appears the pressure generated by the current HydraArchimedes™ tool can be increased to provide better mixing and containment of the cement within its region of displacement in the well, whereby the tool will function as an effective restrictor in the well. The CFD-simulations indicated that the wiping effect from the tool's rubber blades diverts the cement into the annulus due to its rotation. The testing indicated that Impeller 1, which has two blades threaded around its axis at a pitch ratio of 1.5, generates the largest amount of pressure and therefore functions as a very efficient restrictor in the well. Small-scale testing and CFD-simulation also indicated that the optimal cement displacement solution is obtained by connecting an axial flow impeller on top of the HydraArchimedes™ tool.

Table of Contents

Acknowledgement	i
Abstract	ii
Table of Contents	iii
List of Figures	v
List of Equations	vii
List of Tables	viii
List of Abbreviations	ix
1. Introduction	1
1.1. HydraWell Intervention	1
1.2. Plug and Abandonment	1
1.2.1. NORSOK-D010	2
1.2.1.1. Well Barrier	2
1.2.2. Conventional P&A	4
1.2.3. Perforate-wash-cement PWC®	6
2. Test-rig	8
2.1. Modified test-rig	8
2.1.1. Bottom POM-structure	9
2.1.2. Top POM-structure	10
2.1.3. Perforated casing	11
2.1.4. Circulation of water	13
2.1.5. Dye	16
3. HydraArchimedes™ test	18
3.1. HydraArchimedes™ design	18
3.2. HydraArchimedes™ results	18
3.2.1. HydraArchimedes™ pressure test	18
3.2.1.1. HydraArchimedes™ pressure vs RPM	19
3.2.2. HydraArchimedes™ displacement test	19
3.2.2.1. HydraArchimedes™ dye displacement at 50 and 100 RPM	20
3.3. HydraArchimedes™ conclusion	20
4. Theory	21
4.1. Screw propeller history	21
4.2. Factors affecting propeller efficiency	24

4.2.1.	Propeller diameter and RPM.....	24
4.2.2.	Pitch	25
4.2.3.	Pitch ratio	26
4.2.4.	Number of blades	27
4.3.	Axial and radial flow impellers.....	27
5	3D-models	29
5.1	Impellers.....	29
5.1.1	DT 1.5 pitch	30
5.1.2	DT 1.5 pitch with decreased OD	30
5.1.3	DT 1.5 pitch 99.5	31
5.1.4	DT 1 pitch – DT 2 pitch – DT 5.88 pitch	31
5.1.5	QT 2.9 pitch.....	32
5.1.6	ST 1.5 pitch	32
5.1.7	Radial flow impeller.....	33
6	Results and discussion	34
6.1	Pressure	34
6.1.1	Pressure vs RPM.....	34
6.1.2	Ratio vs RPM.....	36
6.1.3	Pitch vs RPM.....	38
6.2	Dye-test	39
6.2.1	Dye-testing at 50 RPM.....	39
6.2.2	Dye-testing at 100 RPM.....	40
6.3	Computational fluid dynamics	42
6.3.1	CFD-analysis HydraArchimedes™	43
6.3.2	CFD-analysis Impeller 1.....	45
6.3.3	New configuration – Impeller 10 x HydraArchimedes™	47
6.3.3.1	Pressure-test MK2 configuration.....	48
6.3.3.2	Dye-test MK2 configuration.....	49
6.3.3.3	CFD-analysis MK2 configuration.....	50
7	Conclusion	52
8	Appendix	54
9	References	55

List of Figures

Figure 1: Permanent abandonment, two back-to-back cement plugs [3].	3
Figure 2: Illustration of internal and external WBE in a well [3].	4
Figure 3: 3-step section milling operation [7].	5
Figure 4: TCP gun fired inside the P&A area [7].	6
Figure 5: HydraWell tool during washing (left) – spacer fluid (middle) – cementing (right) [7].	7
Figure 6: Schematic drawing of test-rig used in this thesis.	8
Figure 7: Test-rig used in this thesis.	9
Figure 8: Bottom POM-structure on the test-rig.	10
Figure 9: Top POM-structure on the test-rig.	10
Figure 10: Perforated plexiglas tube.	11
Figure 11: Showing a 100 mm long illustration of the casing with 60 degrees phasing's.	12
Figure 12: HydraArchimedes™ cement insurance tool.	18
Figure 13: Pressure generated vs different RPMs for the HydraArchimedes™.	19
Figure 14: HydraArchimedes™ dye displacement test – 50 RPM (left) and 100 RPM (right).	20
Figure 15: Archimedes screw transporting water from one level to another [16].	21
Figure 16: Drawing of the world's first submersible vessel, Submarine Turtle [18].	22
Figure 17: Smith's design of the screw propeller [13].	23
Figure 18: Screw propeller on the SS Archimedes ship [13].	23
Figure 19: Propeller diameter [21].	24
Figure 20: Boat propeller pitch visualization [22].	25
Figure 21: Screw pitch [24].	25
Figure 22: Single bladed screw impeller in a draught tube [25].	26
Figure 23: Graph indicating optimal pitch ratio [25].	26
Figure 24: Number of blades on propeller [26].	27
Figure 25: Radial flow pattern (left) and axial flow pattern (right) [28].	27
Figure 26: Pitch blade (left), marine (middle) and hydrofoil (right) [30].	28
Figure 27: Radial flow impeller [31].	28
Figure 28: Impeller 1.	30
Figure 29: Impeller 2.	30
Figure 30: Impeller 3.	31
Figure 31: Impeller 4.	31
Figure 32: Impeller 5.	32
Figure 33: Impeller 6.	32

Figure 34: Impeller 7.	32
Figure 35: Impeller 8.	33
Figure 36: Impeller 9.	33
Figure 37: Pressure generated by different impellers vs RPM. Indicating which impeller generates the largest pressure difference.	35
Figure 38: Ratio vs RPM. Indicating how much more pressure the different impellers generates compared to the HydraArchimedes™ (red baseline).	37
Figure 39: mbar vs pitch ratio for Impeller 1, 4, 5 and 6. Indicates which impeller generates the largest pressure.	38
Figure 40: Dye displacement test at 50 RPM. Injecting dye during water circulation and impeller rotation.	40
Figure 41: Dye displacement test at 100 RPM. Injecting dye during water circulation and impeller rotation.	41
Figure 42: The HydraArchimedes™ cement slurry volume concentration showing displacement of the mud after 7.151 s. Red indicate 100% cement and blue indicate 100% mud [32].	43
Figure 43: Cement concentration plotted on the cross-section in the perforated casing along the lower part of the HydraArchimedes™ after 7.151 s [32].	44
Figure 44: Impeller 1 cement slurry volume concentrations showing displacement of the mud after 7.150 s. Red indicate 100% cement and blue indicate 100% mud [32].	45
Figure 45: Cement concentration plotted on the cross-section in the perforated casing along the lower part of Impeller 1 after 7.150 s [32].	46
Figure 46: Shaft with the MK2 configuration mounted on.	47
Figure 47: Impeller 10.	47
Figure 48: Showing pressure generation vs RPM for four different impeller configurations. .	48
Figure 49: Dye-test at 50 RPM – HydraArchimedes™ (left) and MK2 configuration (right) ...	49
Figure 50: Dye-test at 100 RPM – HydraArchimedes™ (left) and MK2 configuration (right).	49
Figure 51: MK2 configuration cement slurry volume concentrations showing displacement of the mud after 7.15 s, 10 s and 12 s, respectively [33].	50
Figure 52: Cement concentration plotted on the cross-section in the perforated casing along the lower part of the MK2 configuration after 12 s [33].	51
Figure 53: MK2 configuration.	53

List of Equations

Equation 1: Circumference of casing	12
Equation 2: Area of casing	12
Equation 3: Total area of holes	12
Equation 4: Diameter of holes	12
Equation 5: Velocity of the liquid in full-scale.....	14
Equation 6: Velocity of the liquid in scaled model.....	14
Equation 7: Fluid flow in scaled model	14
Equation 8: Fluid flow over the HydraArchimedes™ in full-scale	14
Equation 9: Percentage reduction of flow over the HydraArchimedes™	14
Equation 10: Scaled fluid flow over the HydraArchimedes™	14
Equation 11: Formula for calculating Reynolds Number.....	15
Equation 12: Reynolds Number for this system.....	15
Equation 13: Bernoulli's equation for turbulent flow	15
Equation 14: Friction factor in Bernoulli's equation	16
Equation 15: Height from water tank to outlet.....	16
Equation 16: Formula for calculating ratio	36

List of Tables

Table 1: Real scale and scaled values used through Equations 5-15..... 13

List of Abbreviations

P&A	Plug and Abandonment
PWC®	Perforate-wash-cement
CFD	Computational Fluid Dynamics
PP&A	Permanantly Plug and Abandonment
NCS	Norwegian Continental Shelf
WB	Well Barrier
WBE	Well Barrier Element
POOH	Pulled Out Of Hole
RIH	Run In Hole
BOP	Blow Out Preventer
PAF	Plug and Abandonment Forum
TCP	Tubing Conveyed Perforation
POM	Polyxymethylene
DT	Double Threaded
OD	Outer Diameter
QT	Quadruple Threaded
ST	Single Threaded
WBM	Water-based-mud

1. Introduction

HydraWell Intervention

HydraWell Intervention AS is a Norwegian service company based in Tananger. The company was founded in 2008. In 2009, HydraWell's PWC®-technology was developed and made available for use. With this technique, HydraWell revolutionized the way wells are P&A.

Plug and Abandonment

The intention with this section is to give the reader a brief introduction to how a well is P&A. This part is essential for the thesis, not only because it describes the difference between the conventional way of plugging a well and the new and more efficient PWC®-method invented by HydraWell, but it also gives an understanding of why HydraWell is using the HydraArchimedes™ tool, and why it is beneficial to optimize the tool design.

A petroleum reservoir is a subsurface pool of hydrocarbons stored in porous, or fractured, formations overlain by cap rocks of low permeability. If not trapped by cap rocks, hydrocarbons will rise to the surface because of its density compared to water. To get hold of the "black gold", a well must be drilled through the cap rock and into the reservoir, thereby destroying the natural cap sealing of the hydrocarbons and creating a flow path for production of the hydrocarbons [1]. The well is producing as long as there are hydrocarbons present, or as long as it is profitable. At the end of a well's lifetime, the operators usually have two options; 1) P&A the well permanently or 2) do a slot recovery of the well. Slot recovery means plugging the well above the reservoir and drill a new well into a more productive zone in the reservoir using existing casings above the plug.

P&A is the discipline in the oil and gas industry where the objective is to reestablish the cap rock, preventing hydrocarbons to migrate to the surface after abandoning the well. Leaking oil and gas from abandoned wells can be hazardous for the surrounding environment, and it is a growing global concern. Alone in Norway, there are currently 3000 wells required to be PP&A (permanently plugged and abandoned), and several new wells are planned to be drilled in the future. When operators decide to drill a well they are also committed by the Norwegian Petroleum Safety Authority to P&A the well when it is no longer in use. P&A is an operation that does not generate positive cash flow for the operators, only costs. In fact, Norwegian taxpayers cover 78% of the costs, while the operators cover the rest. Hence, it is in everyone's interest to develop cost-efficient and reliable P&A technology [2].

1.1.1. NORSOK-D010

NORSOK-D010 is a standard that defines requirements and guidelines relating to well integrity in drilling and well activities and is the standard used on the Norwegian continental shelf (NCS). Well integrity means application of technical, operational and organizational solutions to reduce the risk of uncontrolled release of formation fluids throughout the life cycle of a well [3].

Chapter 9 of the NORSOK-D010 presents the standards, requirements and guidelines for P&A operations, which is an important motivation for this thesis because it's focus is on the rock-to-rock sealing. This chapter contains information about both temporary and permanent abandonment, but this thesis will only focus on PP&A. Permanent abandonment is defined as *"a well status, where the well is abandoned and will not be used or re-entered again"* [4].

1.1.1.1. Well Barrier

Well barrier (WB) – An envelope of well barriers that together prevent the fluid to flow unintentionally from the formation and into the wellbore, into another formation or to the external environment.

Well barrier element (WBE) – A physical element that alone does not prevent flow, but in combination with other WBEs creates a well barrier.

NORSOK-D010 says that there should always be at least two WBE in the well, at all time. For P&A operations, this means setting two cement plugs in the well, one primary and one secondary well barrier. The secondary well barrier is set above the primary in case of failure. The regulations for the primary and secondary well barrier are the same. Figure 1 shows an example of two well barriers in a well. The blue color indicates the primary WBE and the red color indicates the secondary WBE. More examples can be found in NORSOK D-010 [3].

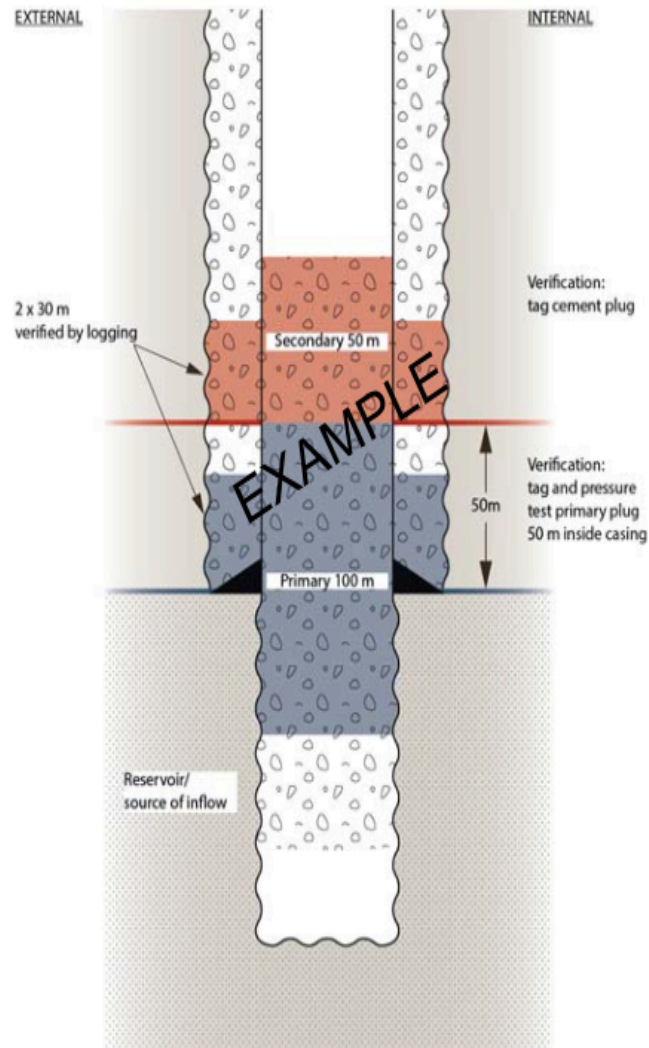


Figure 1: Permanent abandonment, two back-to-back cement plugs [3].

NORSOK-D010 divides the WBE, Figure 2, into an external and internal barrier. NORSOK D-010 states that the requirement for an external WBE (casing cement) shall be 50 m with formation integrity at the base of the interval, or 30 m with adequate bonding if logging verifies the casing cement. The internal WBE shall be placed over the entire interval where there is a verified casing cement and shall be a minimum of 50 m if set on a mechanical plug as a base. Without foundation, the cement plug must be a minimum of 100 m. The well barrier shall also be placed adjacent to an impermeable formation. Permanently abandoned wells shall be plugged with an eternal perspective and must withstand any chemical and geological processes [3].

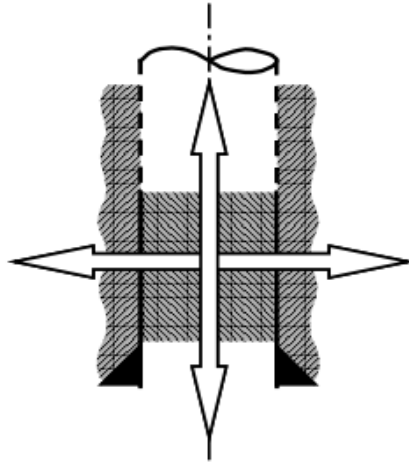


Figure 2: Illustration of internal and external WBE in a well [3].

NORSOK-D010 states that a permanent well barrier should have the following characteristics:

1. *Provide long term integrity (eternal perspective);*
2. *Impermeable;*
3. *Non-shrinking;*
4. *Able to withstand mechanical loads/impact;*
5. *Resistant to chemicals/substances (H_2S , CO_2 and Hydrocarbons);*
6. *Ensure bonding to steel;*
7. *Not harmful to the steel tubulars integrity” [5].*

1.1.2. Conventional P&A

Poor cement behind the casing is something that often appears in wells. When plugging a well, it is essential, as previously discussed, that the WBE extends across the entire cross-section, creating a rock-to-rock seal, to stop the migration of hydrocarbons. When there is no proper hydraulic isolation in the annulus, the conventional way has been to remove the casing over 50 m by section milling to be able to install a rock-to-rock cement plug. After removing the casing and old cement the tool is pulled out of hole (POOH). A cementing tool is then run in hole (RIH), and cement is pumped into the well while the string is POOH [6]. See Figure 3.

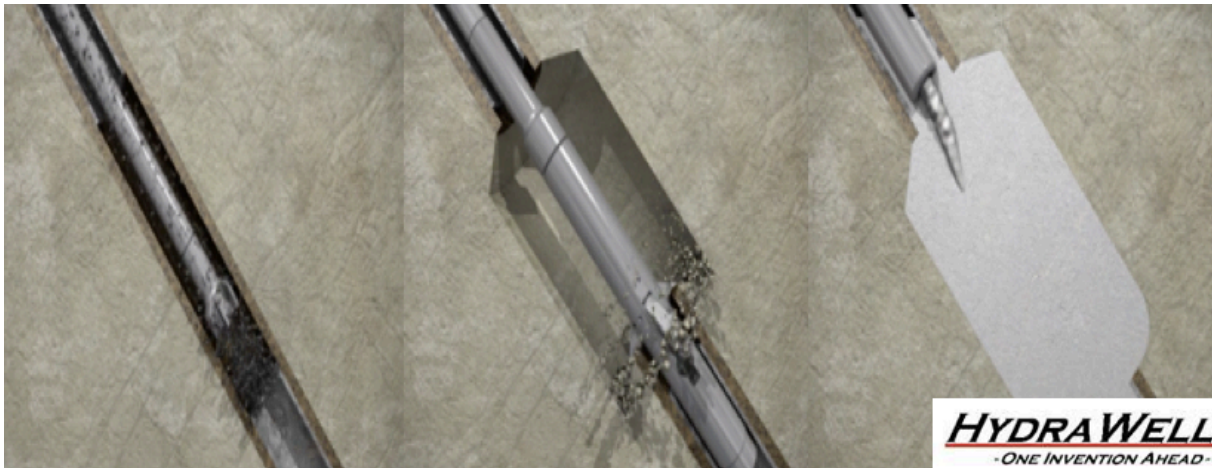


Figure 3: 3-step section milling operation [7].

This multiple-step operation is time consuming and costly because it requires many rig days. A major challenge regarding section milling is the swarf generation. Removing 50 m of 9-5-8" casing generates about 4000 kg of swarf. Swarf generation is bad because it increases the possibility of stuckpipe as well as injuries during swarf handling on the platform. After the milling job, the blow out preventer (BOP) has to be maintained and tested, and often worked over, because swarf piles up the cavities in the BOP on the way to the surface [8].

The plug and abandonment Forum (PAF) has done some cost estimations showing how much it will cost to plug all the existing and upcoming wells on the NCS, using the conventional P&A method:

Assuming there are today 3000 wells to be plugged in the future, and that each well will take approximately 35 days to plug. One rig will therefore P&A 10 wells pr. year. Assuming using 15 rigs, then 150 wells will be P&A pr. year, and to plug 3000 wells using 15 rigs it will take $3000/150 = 20$ years. During these 20 years, PAF has estimated that 144 new wells will be drilled each year. Thus, 2880 new wells will be drilled during the 20 years it will take to P&A the already existing wells, and the 2880 wells will take $2880/150 = 19.2$ years to plug. The conclusion is that 15 rigs will do full time P&A for approximately 40 years. PAF has assumed that each rig cost 300 000 USD/day x 6 NOK = 1.8 mill NOK pr. day, and that the overhead costs for each rig is approximately 2.2 mill NOK pr. day. Which means that the total rate is 4 mill NOK pr. day. This means that the yearly costs pr. rig will be 4 mill NOK x 365 days = 1 460 mill NOK. Assuming 15 rigs are used over 40 years the total cost will be 876 billion NOK. 22 % of these costs are payed by the license holders, while 78 %, or 683 billion NOK, are payed by you and me [2].

1.1.3. Perforate-wash-cement PWC®

As discussed above, there are some significant disadvantages of the conventional way of P&A a well, and the fact that the taxpayers are paying 78 % and the license holders are paying 22 % of the cost, there are strong incentives for developing new technology. As mentioned earlier, a company who took this opportunity and revolutionized the P&A operation was HydraWell Intervention. The main game changer was the PWC®-technology itself, which allows for one-trip operations, thereby saving the operators a lot of money and time.

Another significant advantage of the PWC®-technology is the elimination of the steel swarf removed. As mentioned above, the enormous swarf generation from the conventional method is bad for the BOP and leads to high service costs. The swarf generation must also be handled on the surface, which is a dangerous and time-consuming job. To solve this problem, HydraWell uses a tubing-conveyed perforating (TCP) gun which is installed at the bottom of the tool. The gun is fired when the TCP gun is placed at the P&A depth, creating a perforated zone in the casing which connects the inside of the casing with the annular space on the outside of the casing [9]. See Figure 4.

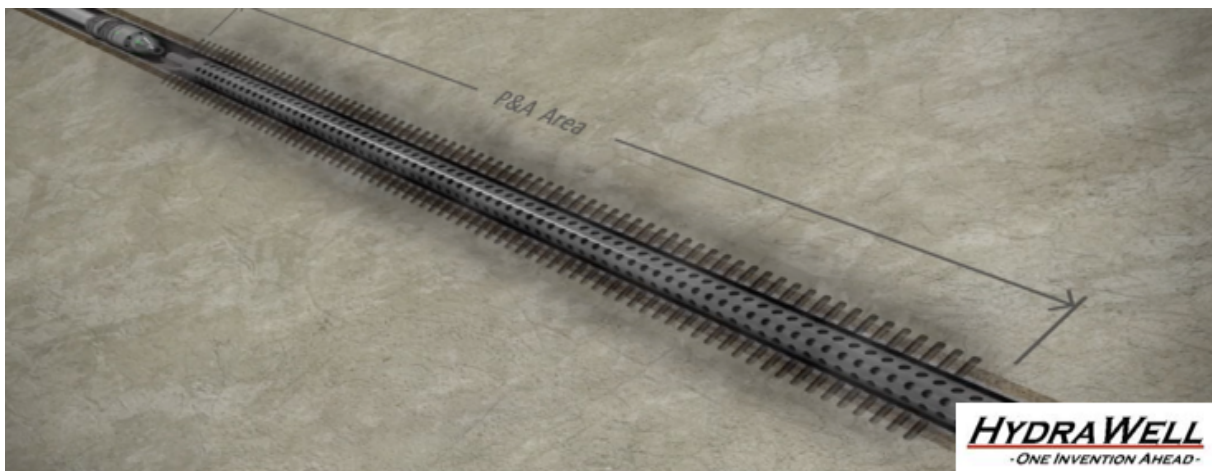


Figure 4: TCP gun fired inside the P&A area [7].

A benefit of the milling process is that all of the debris and old cement is removed, and that the new cement can easily be placed over the entire cross-section, creating a proper rock-to-rock sealing. Since HydraWell is only removing 2 % of the casing goods with the TCP gun, it is much more difficult to gain access to the annular space and ensure the same sealing. However, HydraWell uses high energy jets, which penetrates the perforated holes several times to ensure efficient cleanout in the annular space. See Figure 5.

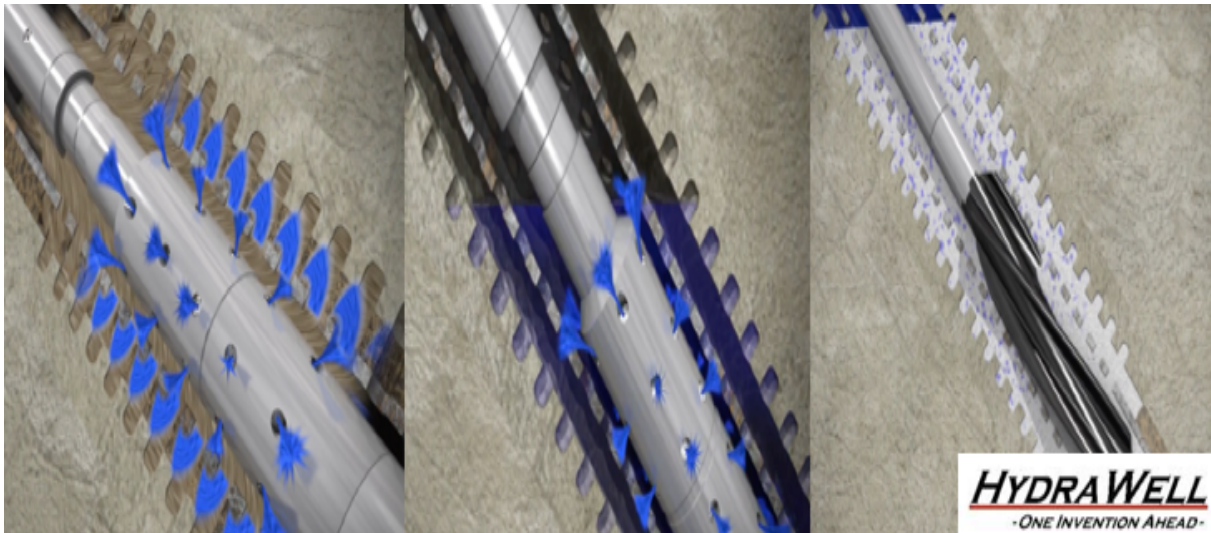


Figure 5: HydraWell tool during washing (left) – spacer fluid (middle) – cementing (right) [7].

After the cleanout and placement of the spacer fluid, cement is pumped out as jets of high energy penetrating the perforations multiple times. At the same time as cement is pumped out and the tool is POOH, the tool rotates at 80-120 RPM. This rotation allows the HydraArchimedes™ tool to rotate at the same speed, as the string it is connected to, which diverts the cement out through the perforated holes. The HydraArchimedes™ is an important tool for HydraWell because it ensures proper displacement of cement into the annular space behind the casing to create rock-to-rock sealing equally good as the conventional method [9].

2. Test-rig

In 2016 Vegard Rongve and Tor Kristian Opaas wrote a Bachelor's thesis for HydraWell Intervention. This thesis was concerned with building a test-rig that could be used to analyze the pressure generated by the 7", 9-5/8" and 13-3/8" HydraArchimedes™ tools. Information regarding the building process can be found in Rongve & Opaas [10]. The following sections contain information regarding further modifications necessary to analyze the annular flow created by the cement insurance tool in the present Master's thesis.

Modified test-rig

Figure 6 is a schematic drawing of the modified test-rig used in this Master's thesis. The different components are labelled to give the reader an understanding of how the modified test-rig works. Water flows from the water tap through hose A and into the water tank B. When the water in the water tank reaches outlet C the ball valve D is opened. The water level in the water tank is maintained stable due to the surplus water flows through hose E and into the return tank F. The water flows from the water tank B through hose G and into the test-chamber H when the ball valve D is opened. The test-chamber H is held in place and positioned between the top I and the bottom J parts of a polymethylene (POM) structure. Each part of the POM-structure is explained in detail in Section 2.1.1 and 2.1.2. A syringe filled with dye is injected into hose G through the injection valve K. The dye follows the water through the hose G and interacts with the impeller L to be tested inside the test-chamber H. The impeller L forces the dye out through the perforations in the casing M and colours the outside of the casing purple. The water and dye then flows out of the test-chamber and into the return tank F through the hose N. Pressure is recorded at the bottom of the test-chamber through hose O which is connected to the pressure transducer P. Figure 7 is a picture of the modified test-rig.

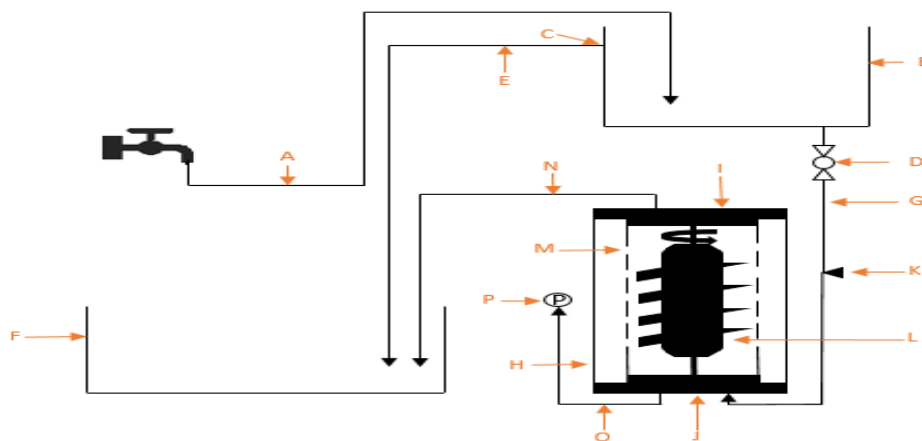


Figure 6: Schematic drawing of test-rig used in this thesis.



Figure 7: Test-rig used in this thesis.

2.1.1. Bottom POM-structure

The bottom POM-structure originally had only a 4 mm hole, which was originally only intended for logging the pressure generated by the HydraArchimedes™ tool, see Rongve & Opaas [10]. However, to circulate water at a scaled rate, see Section 2.1.4, the size of the hole was increased as much as possible, 175 mm². The hole-size was increased by drilling 13 extra 4 mm holes around the top of the bottom POM-structure, see point A on Figure 8. Figure 8 is a 3D-drawing of the modified POM-structure. Water flows from the water tank B and into the test-chamber H through the holes indicated with A in Figure 8.

2.1.3. Perforated casing

To simulate what is happening in the annulus on the outside of the casing, the plexiglas tube itself had to be modified, indicated with an M in Figure 6. To make the scenario as real as possible, it was decided to create the perforated zone a bit longer than the impeller, since in full-scale there are perforated holes over and under the HydraArchimedes™ tool most of the time. As mentioned, approximately 2 % of the casing is removed by the TCP gun in full-scale. This is also the case for the scaled scenario. Perforation holes with 60 degrees phasing and diameter of 4.5 mm, see calculations in Equations 1-4, were printed on an A3 paper and attached around the casing and drilled out. Figure 10 shows the perforated casing.



Figure 10: Perforated plexiglas tube.

The perforated holes were scaled down according to the fact that approximately 2 % of the casing is removed by the TCP gun in a full-scale P&A operation. A 100 mm section of the casing, which includes 25 holes with 60 degrees phasing was used for calculating the perforation diameter. See Figure 11.



Figure 11: Showing a 100 mm long illustration of the casing with 60 degrees phasing's

$$\pi * D_{OD \text{ casing}} = 3.14 * 60 \text{ mm} = 188.4 \text{ mm} \quad (1)$$

$$188.4 \text{ mm} * 101 \text{ mm} = 19028.4 \text{ mm}^2 \quad (2)$$

$$\frac{X}{19028.4 \text{ mm}} = 0.02 \rightarrow X = 0.02 * 19028.4 \text{ mm}^2 = 380.57 \text{ mm}^2 \quad (3)$$

$$r = \sqrt{\frac{380.57 \text{ mm}^2}{\pi * 25}} \text{ mm} = 2.2 \text{ mm} \quad (4)$$

$$d = r * 2 = 2.2 * 2 = 4.4 \text{ mm}$$

2.1.4. Circulation of water

When conducting a P&A operation, as described earlier, HydraWell is pumping cement down into the well usually at a rate of $0.003974 \frac{m^3}{s}$ (63 gpm) for 7" casings. The cement moves down inside the supply tubing and up between the tubing and the casing where the cement engages the HydraArchimedes™ tool. The HydraArchimedes then forces the cement out through the path of least resistance, which is out through the perforations and into annulus. This situation was simulated with the test-rig by allowing water, which simulates mud and cement, to circulate through the test-rig system. To make the situation as realistic as possible, the fluid rate was scaled down to 1/3 of full-scale, which is the same as for the HydraArchimedes™ and the casing. For more information regarding scaling, see Section 5.1. During a full-scale operation, the tool is POOH at 0.03 m/s (6 ft/min) while cementing, implying that less cement is flowing over the HydraArchimedes™ tool [9]. The fluid rate calculations in Equations 5-15 have taken into consideration that the HydraArchimedes™ tool cannot move in the vertical direction in the test-rig. Column 2 in Table 1 contains values based on full-scale 7" casing P&A operation. Column 3 in Table 1 contains values which is scaled based on the values in column 2. The numbers in Table 1 are used in calculations through Equations 5-15.

	Full scale values	Scaled values
Length of impeller	<i>900 mm</i>	$\frac{900}{3} = 300 \text{ mm}$
Diameter of impeller	<i>152.4 mm</i>	$\frac{152.4}{3} = 50.8 \text{ mm}$
ID of casing	<i>154.94 mm (6.1")</i>	$\frac{154.94 \text{ mm}}{3}$ $= 51.64 \text{ mm (2.08")}$
Area of casing	$3.14 * \left(\frac{154.94}{2}\right)^2 = 18845 \text{ mm}^2$	$3.14 * \left(\frac{51.64}{2}\right)^2 = 2093 \text{ mm}^2$

Table 1: Real scale and scaled values used through Equations 5-15.

$$\frac{63 \text{ gal} * m^3 * 1 \text{ min} * 1 \text{ inch}^2}{29.21 \text{ inch}^2 * \text{min} * 264 \text{ gal} * 60 \text{ sec} * 0.0254^2 \text{ m}^2} = 0.21 \frac{m}{s} \quad (5)$$

$$\frac{0.21}{3} = 0.07 \frac{m}{s} \quad (6)$$

$$\frac{3.23 \text{ inch}^2 * 13.38 \text{ ft} * 6.93 * 10^{-3} \text{ ft}^2 * 7.48 \text{ gal}}{\text{min} * 1 \text{ inch}^2 * 1 \text{ ft}^3} = \frac{2.236 \text{ gallons} * 0.003785 \text{ m}^3 * 1 \text{ min}}{\text{min} * 60 \text{ sec}} = 0.000141 \frac{m^3}{s} \quad (7)$$

This means that $0.000141 \frac{m^3}{s}$ (2.23 gpm) has to flow through the test-rig to simulate the real situation in the well. As mentioned above, however the string is POOH at 0.03 m/s (6 ft/min) while cementing, implying that less cement is flowing over the HydraArchimedes™ tool. The Equations 8-10 takes this into account:

$$0.21 \frac{m}{s} - 0.03 \frac{m}{s} = 0.18 \frac{m}{s} \quad (8)$$

$$\frac{0.18}{0.21} = 0.86 = 1 - 0.86 = 0.14\% \text{ reduction} \quad (9)$$

$$0.000141 \frac{m^3}{s} * 0.86 = 1.2126 * 10^{-4} \frac{m^3}{s} \quad (10)$$

Based on these calculations, $1.2126 * 10^{-4} \frac{m^3}{s}$ (1.92 gpm) must flow through the system to simulate the cement operation as realistic as possible. The situation inside the well is very chaotic since the fluid is flowing at a very high rate. Therefore, it was assumed that the fluid flow was turbulent. Equation 11 shows the formula used to calculate the Reynolds Number and Equations 12 shows the Reynolds Number calculated for this system.

$$Re = \frac{\rho D \frac{Q}{A}}{\mu} \quad (11)$$

ρ ($\frac{\text{kg}}{\text{m}^3}$) is the density of the liquid, D (m) is the diameter of the pipe, A (m^2) is the area of the pipe, μ ($\text{Pa} \cdot \text{s}$) is the viscosity of the liquid and Q ($\frac{\text{m}^3}{\text{s}}$) is the flow rate. The viscosity of water at room temperature is $8.9 \cdot 10^{-4} \text{ Pa} \cdot \text{s}$. The fluid flow is turbulent if the Reynolds number is larger than 4000 [11].

$$\frac{1000 \frac{\text{kg}}{\text{m}^3} * 0.015 \text{m} \frac{0.6846 \frac{\text{m}^3}{\text{s}}}{1.76 * 10^{-4} \text{m}^2}}{8.9 * 10^{-4} \text{Pa} * \text{s}} = 11538 \quad (12)$$

The fluid flow was well within the turbulent area since the number calculated in Equation 12 was 11538. Since the fluid flow was turbulent the Bernoulli Equation for turbulent flow, Equation 13, was used to calculate the required height of the water tank to obtain the fluid flow calculated in Equation 10 [12].

$$\frac{Q}{A} = \sqrt{\frac{2 * \Delta P}{\rho * (4f \frac{\Delta x}{D} - 1)}} \quad (13)$$

Q ($\frac{\text{m}^3}{\text{s}}$) is the flowrate, A (m^2) is the pipe area, ΔP (Pa) is the pressure difference between the two ends of the pipe, ρ ($\frac{\text{kg}}{\text{m}^3}$) is the density of the liquid, Δx (m) is the distance of the pipe, D (m) is the diameter of the pipe, and f is the friction factor of the pipe/system.

Since the only unknown factor in Equation 13 is basically the friction factor, the water tank was placed at a height equal to 1.9 m, which resulted in a flow rate of $0.0001 \frac{\text{m}^3}{\text{s}}$ (1.58 gpm). Based on this value the friction factor for the pipe/system was calculated to be $7.50086 \cdot 10^{-4}$. See Equation 14.

$$\frac{\left(\left(\left(\frac{\left(2 * 9.81 \frac{m}{s} * 1.93m \right)}{\left(\frac{0.1 \frac{l}{s}}{1.76 * 10^{-4} m^2} \right)^2} \right) + 1 \right) * 0.015m \right)}{4 * 5m} \quad (14)$$

$$= 7.500879 * 10^{-4}$$

After calculating the friction factor Equation 13 was reorganized and solved with respect to the height h. See Equation 15.

$$\frac{\left(\left(\frac{0.1205 \frac{l}{s}}{1.76 * 10^{-4} m^2} \right)^2 * \left(4 * 7.500879 * 10^{-4} * \frac{5m}{0.015m} - 1 \right) \right)}{2 * 9.81 \frac{m}{s^2}} \quad (15)$$

$$= 2.8m$$

To obtain a circulation rate of $1.2126 * 10^{-4} \frac{m^3}{s}$ (1.92 gpm) the water tank was placed 2.8 m above the outlet of the pipe.

2.1.5. Dye

The most difficult and important part of this project was to examine the annular flow scenario on the outside of the casing. Because water is easy to handle it was decided to use water to simulate the cement and the mud. This was important because multiple tests were performed, and also because the cement density is somewhat similar to that of the mud density (16.3 ppg and 14.5 ppg). However, since the tests were conducted with water, it was impossible to visualize the fluid flow created by the HydraArchimedes™ tool without assistance of a colour additive. This was solved by adding a dye to the water. The dye was potassium permanganate, which is an inorganic chemical compound that dissolves in water into an intensively purple solution. Using a 10 ml syringe the chemical was injected into a plastic tube, which was connected to the water tank and also to the bottom POM-structure. When injected into the tube, the chemical followed the water at a pump rate of $1.2126 * 10^{-4} \frac{m^3}{s}$ (1.92 gpm) into the bottom of the test-chamber. Inside the test-chamber, the flow of fluid and chemical was

counteracted by a pressure generated by the HydraArchimedes™ tool. The pressure thus generated, and the interaction with the HydraArchimedes™ tool, forced the water and the dye out through the perforated holes, thereby colouring the outside of the casing purple. In this manner, different tool designs could be tested and compared with each other.

3. HydraArchimedes™ test

HydraArchimedes™ design

Figure 12 is a scaled 3D-drawing of the cement insurance tool used by HydraWell today, called the HydraArchimedes™ tool. This tool has four blades, where each blade is rotated 90 degrees in the longitudinal direction. The impeller was developed to act on the cement both hydraulically, by generating high/low pressure regimes, and mechanically by providing mechanical displacement. The blade material and blade design were selected to allow the tool to work as a spatula inside the casing, thereby swiping over the perforated holes and forcing the cement to the annular outside of the casing.



Figure 12: HydraArchimedes™ cement insurance tool.

HydraArchimedes™ results

This section contains graphs and pictures obtained from testing of the HydraArchimedes™ tool in the test-rig. Results from the pressure testing are presented in Section 3.2.1, while results from dye displacement are presented in Section 3.2.2.

3.1.1. HydraArchimedes™ pressure test

A pressure transmitter, operable within a pressure range of 0 to 62 mbar, was used in combination with a programmable control unit (PLC) and a computer in order to record and log the pressure in the various tests performed for this thesis. For more information about the pressure transmitter and PLC-unit, see Rongve & Opaas [10].

3.1.1.1. HydraArchimedes™ pressure vs RPM

Figure 13 presents the pressures generated by the HydraArchimedes™ tool. The x-axis indicates the different RPMs, ranging from 50 to 150 RPM, with steps of 10 RPM, while the y-axis indicates the pressures generated, measured in mbar. Each step was tested for two minutes, and each point on the graph was calculated by taking the average value of each interval. As can be seen from the graph, the HydraArchimedes™ tool generates a rather low pressure. A 1 m water column is equivalent to 98.06 mbar and the maximum pressure generated by the impeller equals 0.05 mbar, which is equivalent to a 0.00051 m water column.

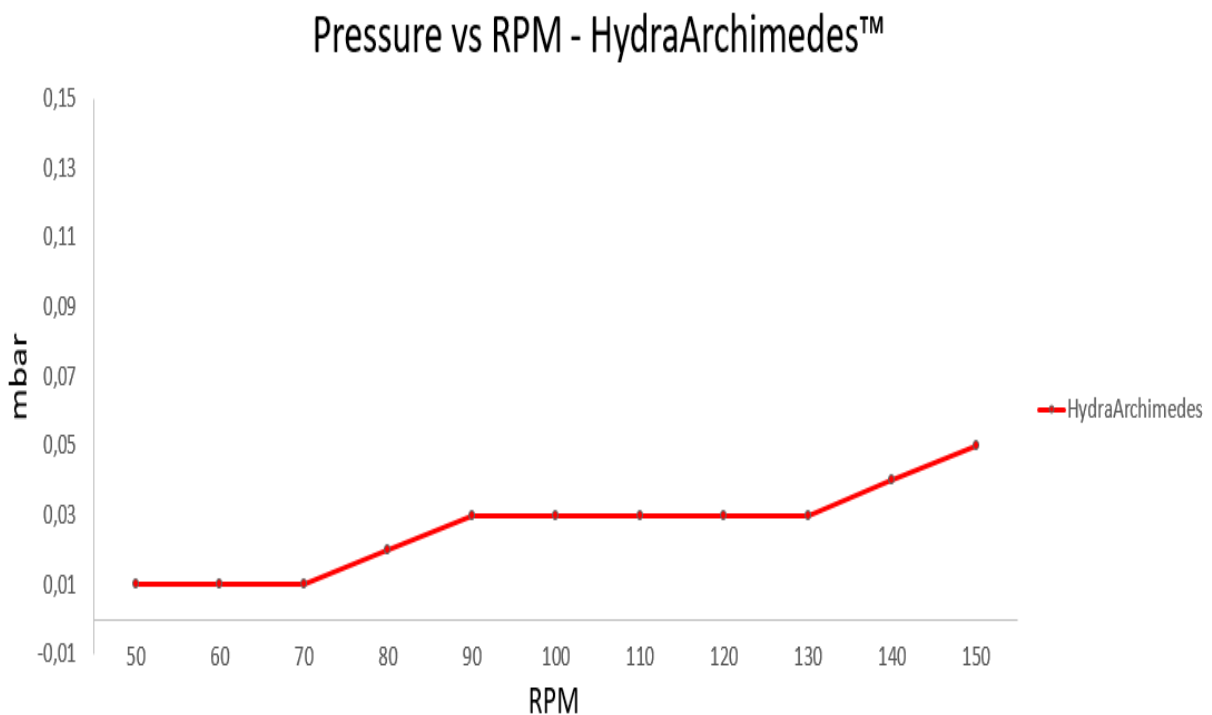


Figure 13: Pressure generated vs different RPMs for the HydraArchimedes™.

3.1.2. HydraArchimedes™ displacement test

In this section, dye was used to visualize the displacement effect on the outside of the casing. Section 3.2.2.1 shows the results obtained from rotating the HydraArchimedes™ tool at 50 and 100 RPM, respectively. For each test, 0.03 g of potassium permanganate was mixed with 10 ml of water before injected. Before each test, a two-minute clear water circulation was carried out to ensure that all of the dye was cleaned out from the outside of the casing. Perfect fluid displacement is indicated with a strong evenly distributed purple color over the perforated area.

3.1.2.1. HydraArchimedes™ dye displacement at 50 and 100 RPM

Figure 14 shows the manner in which the dye is displaced on the outside of the casing using the HydraArchimedes™ tool at 50 and 100 RPM, respectively. Both images were obtained by filming with an iPhone 7, where each film was stopped after four seconds and screenshotted. Dye was injected as explained in Section 2.1.5. It can be seen from Figure 14 that the displacement effect is not optimal because the dye does not cover the whole area of the perforated section of the casing. As mentioned in the introductory part, poor cement displacement behind the casing is critical and may produce channels in the cement through which hydrocarbons can migrate to the surface. Increasing the RPM from 50 to 100 increases the pressure by 0.02 mbar. Figure 14 indicates that dye is spread more efficiently at 100 RPM. Increasing the RPM from 50 to 100 RPM is therefore recommended as it improves the displacement effect slightly. However, the displacement effect is not optimal as the colour intensity is weak and several white spaces can be observed for both pictures in Figure 14.

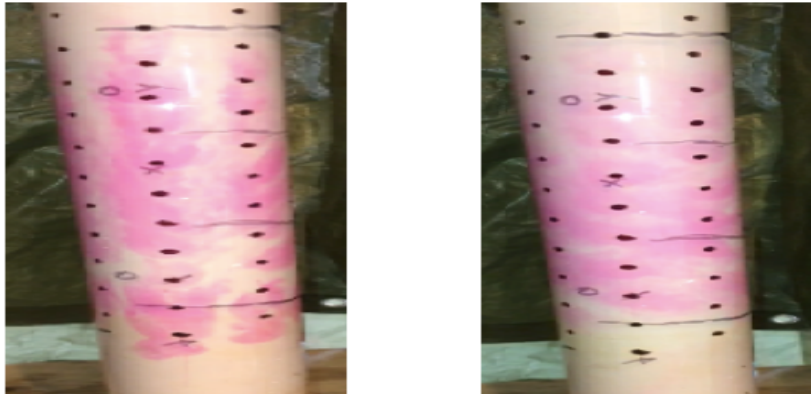


Figure 14: HydraArchimedes™ dye displacement test – 50 RPM (left) and 100 RPM (right).

HydraArchimedes™ conclusion

Based on the pressure and displacement tests presented in this section it is clear that the HydraArchimedes™ design can be improved to increase the cement displacement efficiency of the tool. It is, however, important to take into consideration that the material used in these tests are not the same as in a realistic situation in a well. Also, the available 3D-printer could not print with rubber, whereby the scaled HydraArchimedes™ tool had to be printed in plastic. The spatula effect of the tool was therefore not tested in this section.

4. Theory

With a goal to improve the dye displacement effect of the HydraArchimedes™, boat propeller theory is presented in this chapter and was used as a guideline when redesigning the HydraArchimedes™ in Chapter 5.

Screw propeller history

A propeller is a rotating object consisting of one or more blades attached to a hub. The propeller transforms a rotating motion into thrust force. A pressure difference is produced between the forward and rear surfaces of the shaped propeller blade, and fluid, such as water or air, is accelerated behind the propeller [13].

The propeller design goes way back to before Christ (BC), to the time when the Greek mathematician, physicist, engineer, inventor and astronomer Archimedes lived. Archimedes was born in 287 BC and died 75 years old, during the Second Punic War. He is generally considered the greatest mathematician of antiquity and is one of the greatest inventors of all time. One of Archimedes' most famous inventions are the Archimedes screw [14]. The Archimedes screw is a machine consisting of a tube with a rod on its inside. A blade is threaded multiple times around the rod, see Figure 15. The main purpose of the Archimedes screw is to pump and lift water from one level to another, for example for irrigation purpose. The blade has the function of a channel. When the helix-shaped blade rotates, the water is lifted up to the top of the tube. There are many different stories about why Archimedes made the Archimedes screw. One of the stories is that he saw a woman collecting water from a river then thought there had to be a more efficient way to collect water [15].

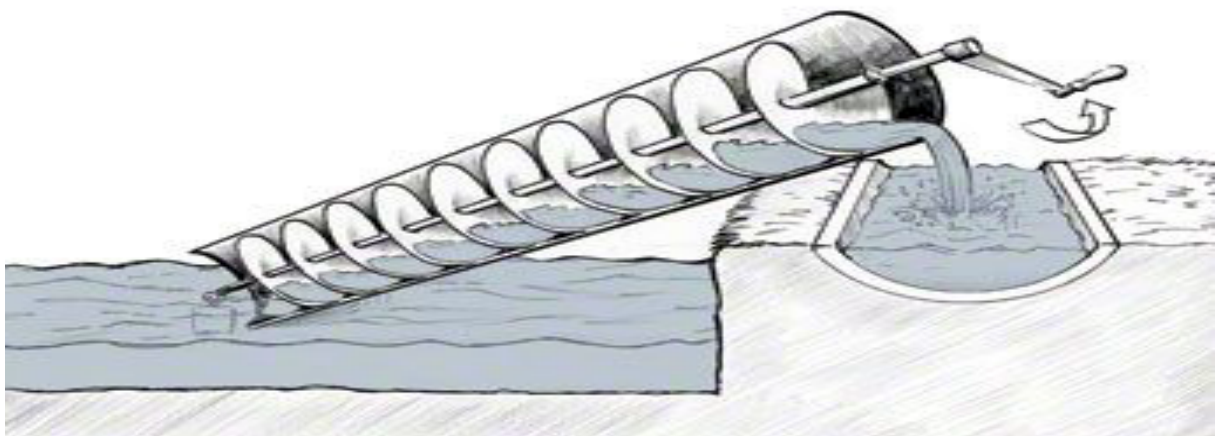


Figure 15: Archimedes screw transporting water from one level to another [16].

The first use of a screw propeller on a watercraft was on the world's first submersible vessel with a documented record of use in combat, called the Turtle. See Figure 16. The submarine was built in 1775 by American David Bushnell. Bushnell understood that the Archimedes screw had the potential to move water in a way that it could create thrust for his submarine. Bushnell installed two screw propellers on his submarine, one to move the submarine in the horizontal direction and one to move it in the vertical direction [17].

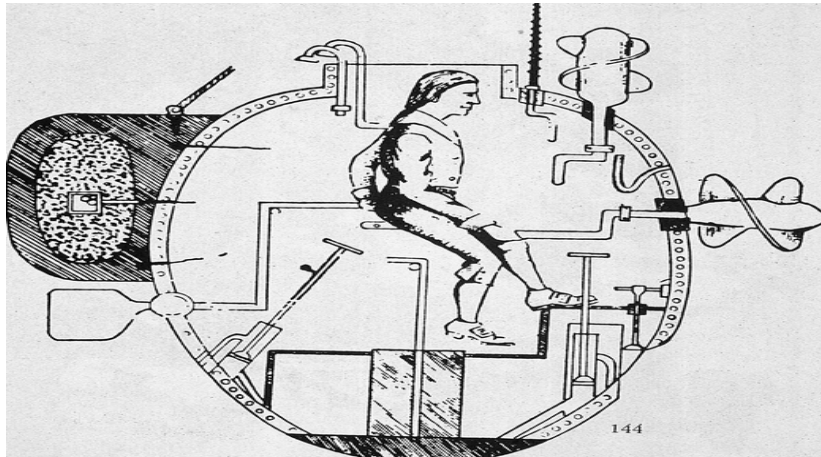


Figure 16: Drawing of the world's first submersible vessel, Submarine Turtle [18].

There was much experimentation with the screw propeller until the 1830s, but almost every single experiment proved unsatisfactory for one reason or another. In 1835, John Ericsson, a Swedish-American inventor, and Francis Pettit Smith, an English inventor, began working separately on the screw propeller problem [13].

Smith was the first person to file a patent on his screw propeller design, while Ericsson filed his patent later. Smith quickly built a small model boat to test his invention, which was demonstrated at the Royal Adelaide Gallery of Practical Science in London, where it was seen by the Secretary of the Navy. After securing the patent, Smith built a 30-foot 6-horsepower boat, which was fitted with a wooden propeller of his own design and tested on the Paddington Canal. Smith's design consisted of a rod with a single blade threaded around its axis two times, 720 degrees. See Figure 17. By accident, the boat hit something in the sea which damaged the propeller. Instead of two turns, the propeller now consisted of only one single turn. To Smith's surprise, the speed doubled, from four miles to eight miles an hour [13].

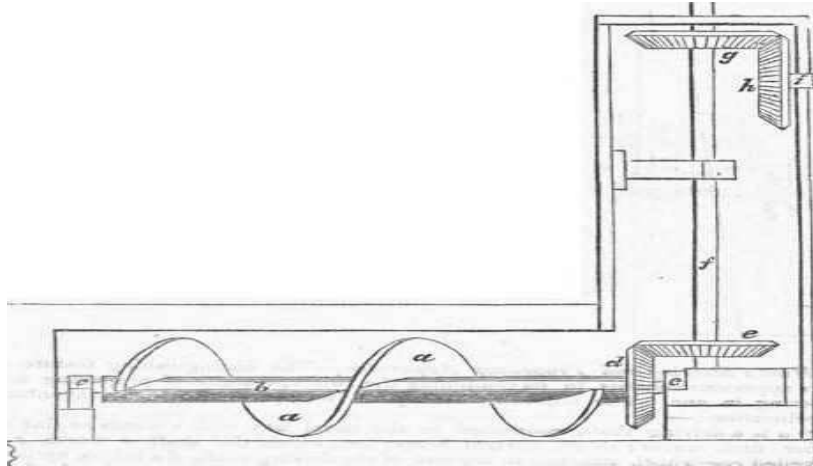


Figure 17: Smith's design of the screw propeller [13].

At the same time, Ericsson built a 45-foot screw propelled steamboat. The boat was demonstrated on the River Thames to members of the British Admiralty. In spite of achieving 10 miles an hour, the members were not impressed. They maintained their view that screw propellers would not be efficient in ocean-going service, and that it would not be steered efficiently. To prove the British Admiralty wrong, Ericsson built a larger ship and sailed to the United States in 1839. He was soon to gain fame as the designer of the U.S Navy's first screw-propelled warship, USS Princeton [13].

Well aware of the British army's view on the screw propeller Smith decided to change it. Smith took his vessel to sea, steaming from Blackwall, London to Hythe, Kent. On his way back, he was observed moving forward in stormy seas by members of the Royal Navy. SS Archimedes was then built in 1838 for the Royal Navy and was the world's first steamship to be driven by a screw-propeller [13]. See Figure 18.

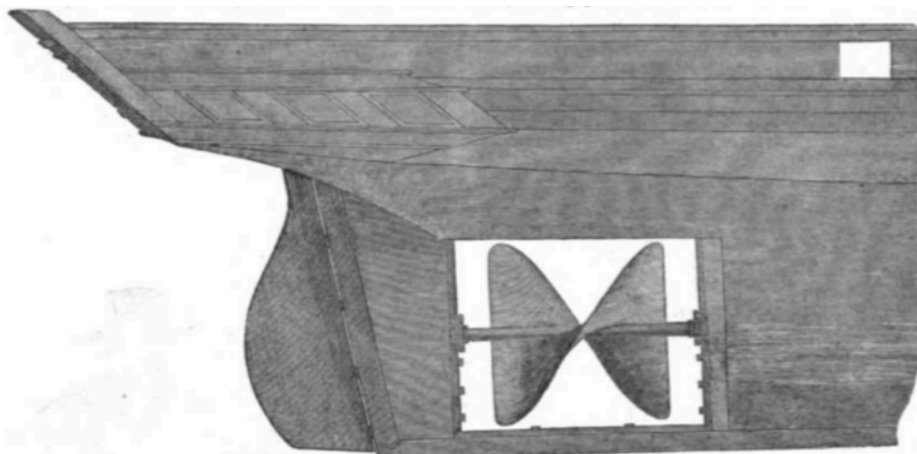


Figure 18: Screw propeller on the SS Archimedes ship [13]

Factors affecting propeller efficiency

A propeller is the last part of the engine, and it is the part of the boat that transfers the power from the engine to the water, creating thrust. To get the most out of the boat engine, an optimized propeller design is crucial. The six most important factors to consider when designing a propeller is: pitch, RPM, diameter, number of blades, blade outline, chamber & angle of attack [19]. For this thesis, only the propeller diameter, RPM, pitch and number of blades will be discussed.

4.1.1. Propeller diameter and RPM

The diameter of the propeller is measured by the diameter of the circle that the blade tips make when rotating, see Figure 19. The propeller works by trapping an amount of water in front of it and then pushing the water backwards, thereby creating forward thrust. This concept follows Newton's third law: if an object A (propeller) exerts a force on an object B (water), then object B must exert a force of equal magnitude and opposite direction back on object A. The larger the propeller diameter, the more water is pushed back and thus allowing the propeller to generate more thrust, hence making the propeller more efficient [20].

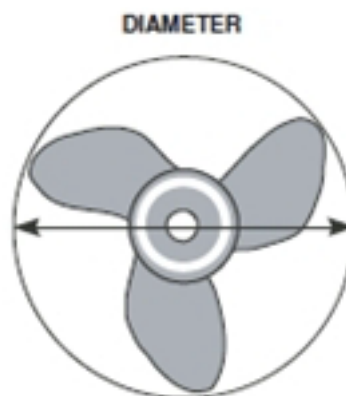


Figure 19: Propeller diameter [21].

The downside of increasing propeller diameter is an increase in the load on the engine and on the shaft. The increased diameter also reduces the final speed because large blades increase drag and the friction forces. Therefore, a large propeller diameter is more efficient at low to medium RPMs, while a smaller diameter is more efficient at high RPMs.

4.1.2. Pitch

The propeller pitch of a boat dictates the propeller displacement resulting from one complete rotation of 360 degrees in a solid material. Since the propeller is not rotating in a solid material, some slip will occur. Slip is the difference between theoretical displacement and the actual displacement of the propeller. A propeller of 21" pitch will advance 21 inches for every complete rotation as long as this is done in a solid material [22]. See Figure 20 for visualization.

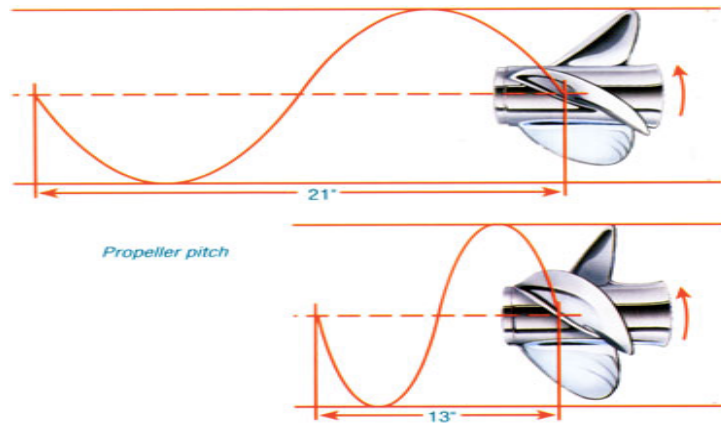


Figure 20: Boat propeller pitch visualization [22].

Determining the best pitch depends on the specific application. A small pitch will cause a boat to accelerate faster but will decrease the top speed as the boate engine will reach its maximum RPM at a slower speed. Oppositely, a larger pitch will cause the boat to go faster but will decrease its acceleration. Hence, it is desirable to find the optimal pitch for the specific application [22].

The pitch concept is used both for propellers and screws. The definition of pitch for a screw is the axial distance covered per thread or screw groove. Rotating a screw 360 degrees with a screwdriver into a wooden-panel will make the screw move into the wall by a length equal to the pitch for a single threaded screw [24]. See Figure 21.

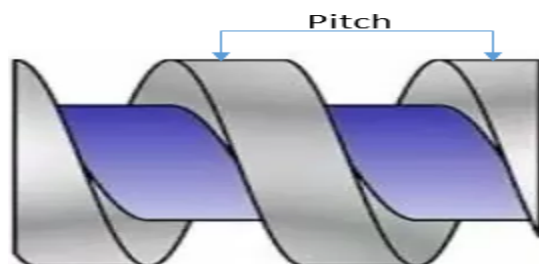


Figure 21: Screw pitch [24].

4.1.3. Pitch ratio

To obtain the best propulsive efficiency for a given propeller diameter, an optimal pitch diameter ratio must be found. Pitch ratio is the relationship between the propeller's pitch and diameter and it is calculated by taking the pitch divided by the diameter (S/d). Yeng-Yung Tsui, a professor at the National Chiao Tung University in Taiwan, has discovered that the maximum flow rate for a helical screw impeller with a single blade is obtained if using a pitch ratio equal to 1.5. Figure 22 shows a screw impeller inside a tube which is placed inside a tank. Figure 23 shows a graph indicating that the maximum flow is obtained at a pitch ratio equal to 1.5 [25].

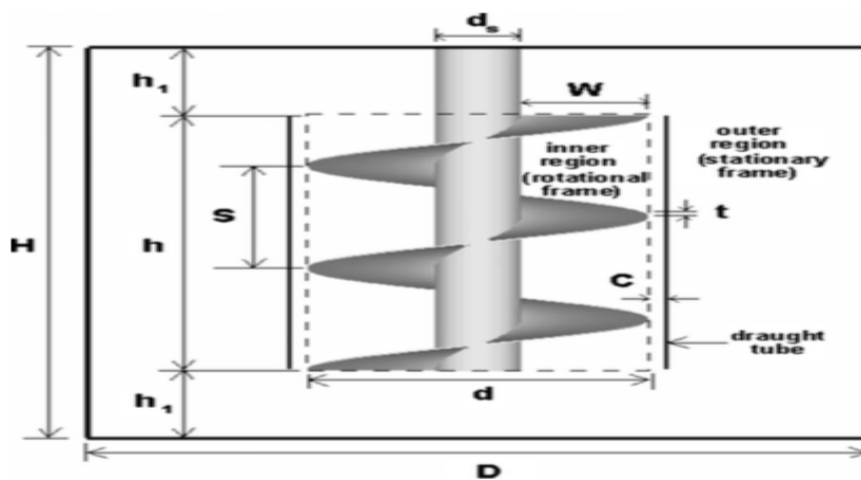


Figure 22: Single bladed screw impeller in a draught tube [25].

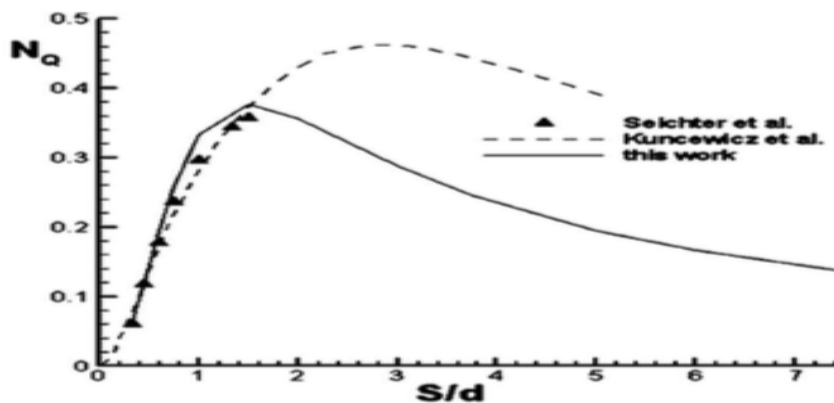


Figure 23: Graph indicating optimal pitch ratio [25].

4.1.4. Number of blades

Propellers can be manufactured with a different number of blades, usually 2, 3, 4, 5 or 6 blades. The highest propeller efficiency is obtained using only one single blade. For strength and vibration reasons however, several blades are generally used. The propeller efficiency generally decreases with increasing number of blades together with unwanted vibration [26]. See Figure 24. The number of blades selected is therefore a crucial factor when designing a propeller.



Figure 24: Number of blades on propeller [26].

Axial and radial flow impellers

Impellers are used in mixing tanks for a wide variety of industries and unique applications. The purpose of an impeller is to transfer power provided by a motor to a substance in the most efficient way in order to produce a desired agitation effect in the least amount of time. When impellers are rotated, they create fluid flow and a flow pattern depending on the particular impeller type used. Axial (down and up) and radial (side to side) flow patterns are most commonly used for mixing purposes [27]. See Figure 25.



Figure 25: Radial flow pattern (left) and axial flow pattern (right) [28].

Axial flow impellers essentially impose bulk motion and are used in homogenization processes where increased fluid flow rate is important. The most common types of axial flow impellers are pitched blade, marine, and hydrofoil impellers [29]. See Figure 26.

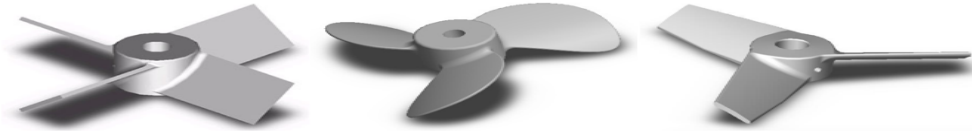


Figure 26: Pitch blade (left), marine (middle) and hydrofoil (right) [30].

Radial flow impellers essentially impose shear stress and are used, for example, to mix very viscous fluids. Such an impeller is usually designed with four to six blades that move the fluid perpendicular to the impeller. See Figure 27. The radial impeller is designed to move the substance (e.g. viscous fluid) in the center of the tank to the sides of the tank, where the substance is forced to move up or down in the tank [29]. See Figure 25.

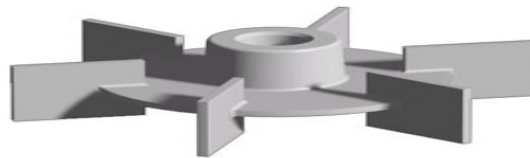


Figure 27: Radial flow impeller [31].

5 3D-models

5.1 Impellers

In this thesis, the name impeller is a collective term for the cement insurance tool used by HydraWell Intervention. This name will be used frequently throughout the thesis, along with the name HydraArchimedes™. In this chapter, nine different impeller 3D-models are presented. Each model was developed based on the theory and concepts in Chapter 4, as well as on the HydraArchimedes™ geometry. In order to understand the results presented in Chapter 6, it is important for the reader to visualize the different impeller designs described in this Chapter 5.

The impeller used today by HydraWell is made out of rubber. The rubber is melted inside a mold made out of steel. The mold are reused many times, but only for one certain design. In order to test a new impeller design, Hydrowell therefore must build an entirely new mold and test it in real scale, which is a very expensive and time-consuming process. To avoid these substantial costs, a 3D-printer was used in this thesis to create scaled impellers made from plastic. In this manner, even very complex impeller designs can be manufactured at a low cost compared to that of real scale impellers. For example, a 7" scaled 3D-printed HydraArchimedes™ tool costs NOK 700, implying that HydraWell can produce and test hundreds of different impeller designs for the price and time of manufacturing only one full-scale impeller.

The impeller used by HydraWell today is 1 m long and exist in four different ODs, 7", 9-5-8", 10-3-4" and 13-3-8". The height of this impeller was a problem for the 3D-printer due to its maximum print height of 400 mm. The OD of the impeller also exceeded the OD of the available plexiglas tubes. It was therefore decided to scale the 3D-printed impeller to approximately 1/3 of the full-scale impeller, which fitted perfectly into the 3D-printer chamber and within the available plexiglas tube. For more information about the scaling, see Rongve & Opaas [10]. The focus in this thesis is primarily on the 7" HydraArchimedes™ tool.

5.1.1 DT 1.5 pitch

Figure 28 is a 3D-drawing of the DT (double threaded) 1.5 impeller. DT implies that two impeller blades are threaded around a cylinder, and 1.5 indicates that the blade pitch ratio is 1.5. The main reason for developing this impeller design was to create an impeller capable of producing the highest pressure possible within the selected RPM envelope (50-100 RPM) based on the theory and concepts presented in Chapter 4. Considering that the impeller is exposed to extreme conditions within the well, whereby a broken impeller could delay well operations for hours or days, two blades were used in this impeller configuration in order to (1) improve the impeller strength and (2) cause less vibration. This impeller is referred to as Impeller 1.

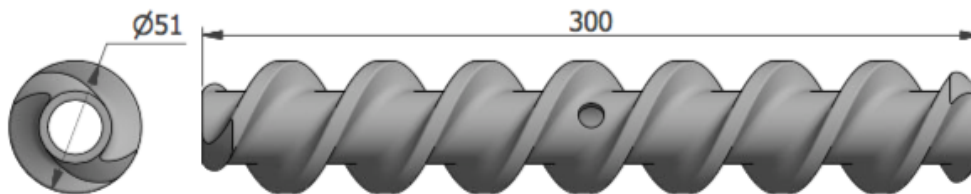


Figure 28: Impeller 1.

5.1.2 DT 1.5 pitch with decreased OD

Figure 29 is a 3D-drawing of the DT 1.5 impeller with a smaller OD, reduced by 4.23 mm. The reduced OD is equivalent to 12.7 mm (1/2") in full-scale. As mentioned earlier, the extreme conditions within a well can be detrimental to the impeller performance and life time. It was therefore decided to test the displacement effect of an impeller having a somewhat reduced OD. Which, in theory, will not engage the casing wall to the degree and therefore will have a longer lifetime and a reduced risk of downtime. This impeller is referred to as Impeller 2. The effect of reducing the OD can be measured by comparing the results of Impeller 2 with the results of Impeller 1 in Chapter 6.

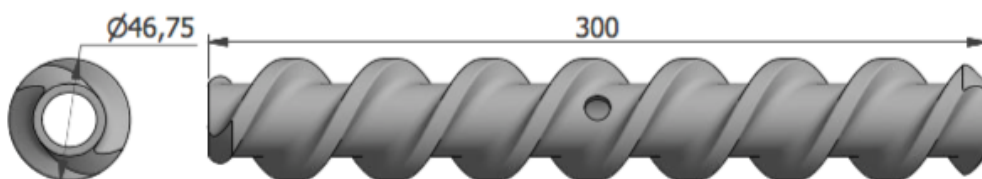


Figure 29: Impeller 2.

5.1.3 DT 1.5 pitch 99.5

Figure 30 is a 3D-drawing of the DT 1.5 pitch 99.5 impeller. This impeller is similar to Impeller 1, however has an impeller length of only 99.5 mm. When HydraWell invented the HydraArchimedes™ tool, they did not investigate the effect of the impeller length on the tool efficiency. If optimizing the impeller length relative to the original 1 m impeller, HydraWell could potentially save money on impeller material. It was therefore decided to manufacture the DT 1.5 pitch 99.5 impeller, which can be compared to Impeller 1 because of the same geometry. This impeller is referred to as Impeller 3.

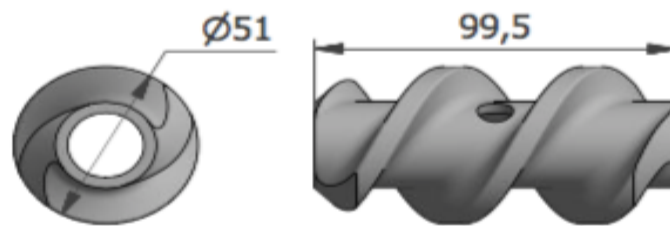


Figure 30: Impeller 3.

5.1.4 DT 1 pitch – DT 2 pitch – DT 5.88 pitch

This section discusses three different impellers. The only difference between these impellers is their pitch ratio. Figure 31 is a 3D-drawing of the DT 1 pitch impeller, which has a pitch ratio of 1, Figure 32 is a 3D drawing of the DT 2 pitch impeller, which has a pitch ratio of 2 and Figure 33 is a 3D-drawing of the DT 5.88 pitch impeller, which has a pitch ratio of 5.88. The main reason for developing these impellers was to check the optimal pitch ratio theory presented in Chapter 3, which stated that the maximum flow is generated at a pitch ratio equal to 1.5. These impellers are referred to as Impeller 4, 5 and 6, respectively.

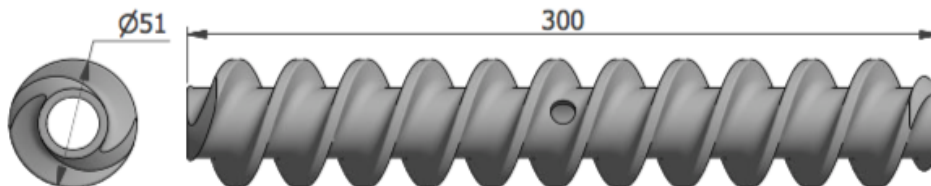


Figure 31: Impeller 4.

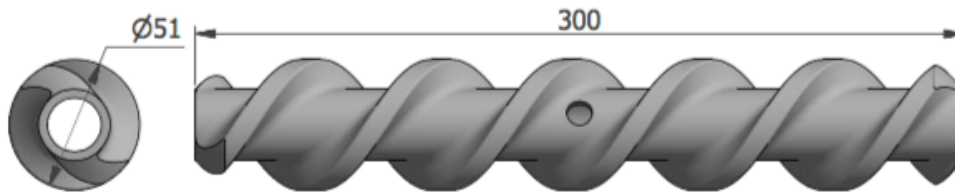


Figure 32: Impeller 5.

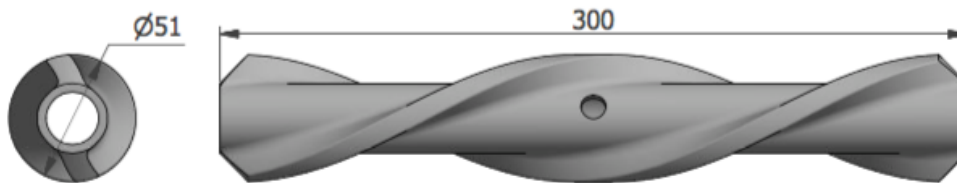


Figure 33: Impeller 6.

5.1.5 QT 2.9 pitch

Figure 34 is a 3D drawing of the QT (quadruple threaded) 2.9 pitch impeller, which has four blades threaded around its axis, each blade having a pitch ratio of 2.9. This Impeller can be compared to Impeller 1 because they both have the same blade area in total. The reason for manufacturing this impeller was to test the combining effect of increasing both the pitch ratio and the number of blades. This impeller is referred to as Impeller 7.



Figure 34: Impeller 7.

5.1.6 ST 1.5 pitch

Figure 35 is a 3D-drawing of the ST (single threaded) 1.5 pitch impeller, which has only one blade threaded around its axis with a pitch ratio of 1.5. The reason for testing this design was to check the theory about number of blades presented in Section 4.2.4. This was conducted by comparing the results with Impeller 1. This impeller is referred to as Impeller 8.

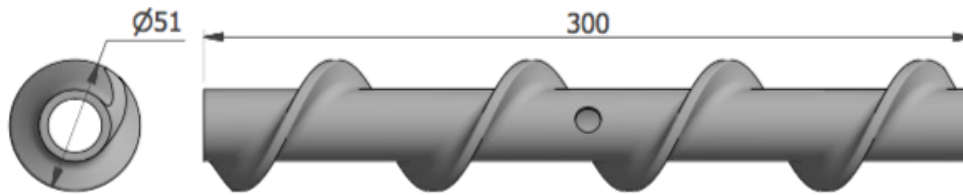


Figure 35: Impeller 8.

5.1.7 Radial flow impeller

Figure 36 is a 3D-drawing of the radial flow impeller. This impeller has five straight axially aligned blades placed around the cylinder with equal space between them. The idea with this design was to check the fluid displacement efficiency for a radial flow impeller. Since this impeller does not have any pitch, pressure will therefore not be generated and logged. Only the fluid flow behind the casing is interesting for this specific impeller design. This impeller is referred to as Impeller 9.

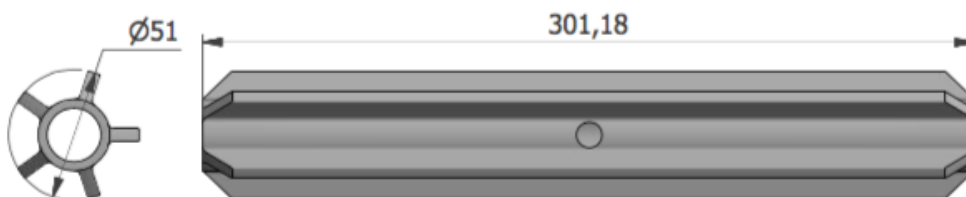


Figure 36: Impeller 9.

6 Results and discussion

This chapter presents graphs and pictures obtained from testing of the impellers presented in Chapter 5. Results from pressure testing are presented in Section 6.1, while results from dye displacement are presented in Section 6.2. The main objective of this chapter is to compare and discuss the performance of the different impeller designs to the performance of the HydraArchimedes™ tool and explain the manner in which were obtained. Appendix 1 provides an overview of the impellers presented in Chapter 5. It is recommended to use this overview as a support when reading Chapter 6.

6.1 Pressure

When rotating an axial impeller clockwise in a fluid, the impeller will try to push the fluid by exerting a certain pressure on it. Impeller geometry and RPM are important factors for the amount of pressure the impeller can generate. In this section, different impeller geometries and RPMs are tested to observe which design and rotational speed generates the highest amount of pressure difference. As in Chapter 3, a pressure transmitter, PLC-unit and a computer was used to record and log the pressures.

6.1.1 Pressure vs RPM

A presentation of pressure vs RPM for the different impellers is shown in Figure 37. Each impeller was tested from 50 RPM to 150 RPM, in steps of 10 RPM, and each RPM was tested for two minutes. Each point on the graph was calculated by taking the average pressure values at each step.

The graph shows large pressure differences between the various impellers. The main purpose of this graph is to range the impellers from worst to best, based on the pressure generated. Each coloured line in Figure 37 indicates an impeller. The red line at the bottom indicates the impeller that generated the lowest amount of pressure, while the blue line on the top indicates the impeller that generated the largest amount of pressure. The graph clearly indicates that the HydraArchimedes™ tool generated the lowest amount of pressure for any given RPM. Impeller 1, which is the impeller that generated the largest amount of pressure, generated 0.47 mbar more pressure than that of the HydraArchimedes™ tool at 80 RPM, and 1.6 mbar more at 150 RPM.

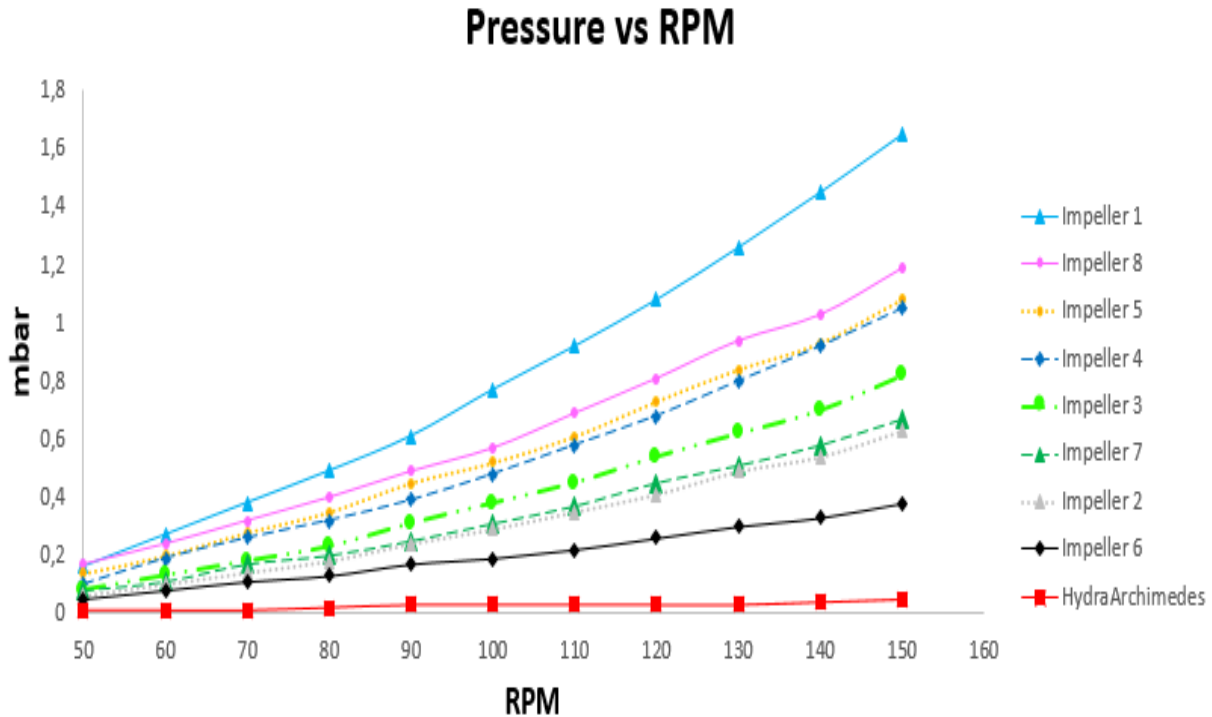


Figure 37: Pressure generated by different impellers vs RPM. Indicating which impeller generates the largest pressure difference.

The graph indicates that the HydraArchimedes™ tool generated almost the same amount of pressure for every single RPM step from 50 to 150 RPM. Impeller 1, which is indicated by the blue line, experienced large pressure differences from 50 to 150 RPM. At 50 RPM, the impeller generated 0.16 mbar and for 150 RPM the impeller generated 1.65 mbar, amounting to a pressure difference of 1.49 mbar. One of the intentions regarding the HydraArchimedes™ tool was to create a restrictor in the well capable of leading the fluid along a path of least resistance, which would be out through the casing perforations and into the annulus. In order for the HydraArchimedes™ tool to function as a restrictor inside the casing, it has to generate a significant amount of pressure. Based on the results shown in Figure 37, it appears the HydraArchimedes™ tool is generating the lowest pressure response. The results also indicated that increasing the RPM of the tool did not improve its efficiency; see the near horizontal red line. Figure 37 also shows that Impeller 1 appear to be the most efficient restrictor as it generates the most pressure at any given RPM, except at 50 RPM. At this point Impeller 8 generated the largest amount of pressure.

The fact that Impeller 1 generated the largest amount of pressure was an interesting observation. This is found to coincide with the theory presented in Chapter 4 stating that the highest propeller efficiency was obtained with only one single blade. Adding several blades to

the propeller increases the friction between the propeller and the water, which results in increased power output from the engine. The impeller on HydraWell's PWC® tool is not intended to push the tool in any direction. The friction in this context is therefore of no significance. Therefore, adding an extra blade to the impeller in this case increases its efficiency.

6.1.2 Ratio vs RPM

Figure 38 is a graph of the same impellers shown in Figure 37. The graph shows the increased efficiency of each impeller as compared to the efficiency of the base, HydraArchimedes™ tool, which is shown as the red baseline. Each data point was calculated as the ratio of the HydraArchimedes™ tool. This is the reason why each data point on the red line equals one, because the number is just divided by itself. Equation 16 provides an example of how the data points were calculated at 150 RPMs. Point 33 at 150 RPM on the blue line was calculated by dividing the average pressure of Impeller 1 by the average pressure of the HydraArchimedes™ tool.

$$\frac{\text{average pressure at 150 RPM for Impeller 1}}{\text{average pressure at 150 RPM for the HydraArchimedes™}} = \text{ratio} \quad (16)$$

This number indicates that Impeller 1 generated 33 times more pressure than that of the HydraArchimedes™ tool at 150 RPM. From the graph, it can be seen that the values of Impeller 8 are below the values of Impeller 1 at all times, except at 50 RPM. The reason for this is not known exactly but could be that Impeller 8 did not operate efficiently at low RPMs, or it could be an error in the reading. However, it is very interesting to observe that the lines in the graph are not linear. The values increase from 50 to 70 RPM, decrease from 70 to 90 RPM, increase from 90 to 130 RPM and decrease again from 130 to 150 RPM. There are clear peaks at 70 and 130 RPM. At these two points, Impeller 1 was 38 times and 42 times more efficient than the HydraArchimedes™ tool. The graph indicates that the impeller had to rotate at 125 RPM to achieve the same ratio as that achieved at 70 RPM. This observation applies to all the impellers and shows a clear trend.

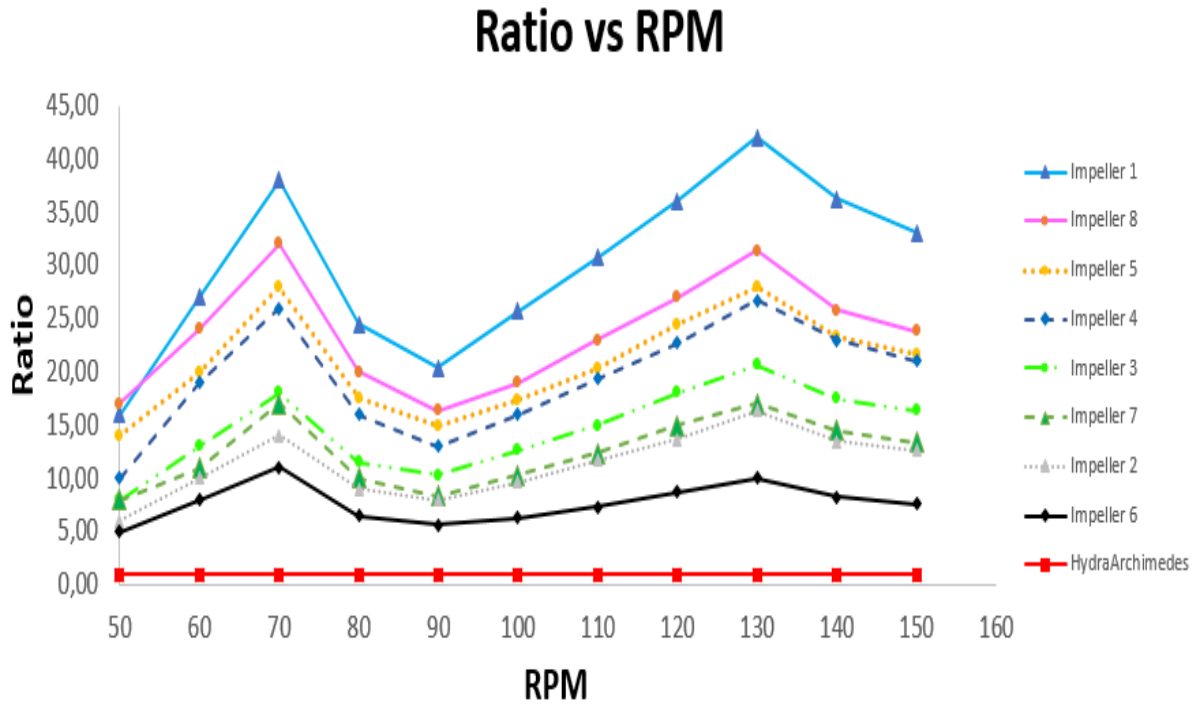


Figure 38: Ratio vs RPM. Indicating how much more pressure the different impellers generates compared to the HydraArchimedes™ (red baseline).

During a P&A operation, HydraWell can rotate the HydraArchimedes™ tool from 0 to 150 RPM. As mentioned in Section 6.1.1, Figure 37 shows that the rotational speed has little effect on the pressure generated by the HydraArchimedes™ tool. Based on Figure 38, the rotational speed has a substantial effect on the pressure generated by the impellers presented in Chapter 5 as compared to the HydraArchimedes™ tool. HydraWell usually rotates the HydraArchimedes™ between 80-120 RPMs. If using any of the impeller designs presented in Chapter 5, Figure 38 indicates that HydraWell could benefit from rotating the tool at 70 to 130 RPMs, as clear efficiency peaks are detected at the corresponding RPMs. Operating Impeller 1 at 130 RPM achieved the best efficiency as compared to the efficiency of the HydraArchimedes™ tool. At this RPM value, Impeller 1 generated 42 times more pressure than that of the HydraArchimedes™ tool.

The yellow line in Figure 37 and 38 shows the performance of Impeller 2. The only difference between Impeller 1 and Impeller 2 was the decreased OD, see Section 5.1.2. The differences in performance between these two impellers are significant. Figure 37 shows that, at 70 RPM, the difference is 0.24 mbar and, at 150 RPM, the difference is 1.06 mbar. This difference increases as RPM increases. Based on these tests, it is therefore recommended to use Impeller 1 for any given RPM. For low RPM operations however, Impeller 2 may be used since the performance difference is small.

6.1.3 Pitch vs RPM

Figure 39 is a graph which represents four different double treaded impellers, where each impeller was rotated at 70 RPM for two minutes. The only difference between the impellers was the pitch ratio. Each point in Figure 39 was calculated by taking the average value of the intervals as in Figure 37. The intention of this graph is to evaluate the importance of the pitch ratio on impeller pressure efficiency, and to test the theory presented in Chapter 4. Value 0.39 represents Impeller 4, value 0.49 represents Impeller 1, value 0.45 represents Impeller 5, and value 0.17 represents Impeller 6. The corresponding pitch ratio values are presented on the x-axis. The graph clearly indicates that the pressure increases with increasing pitch ratio up to 1.5, and then the pressure decreases with further increasing pitch ratio.

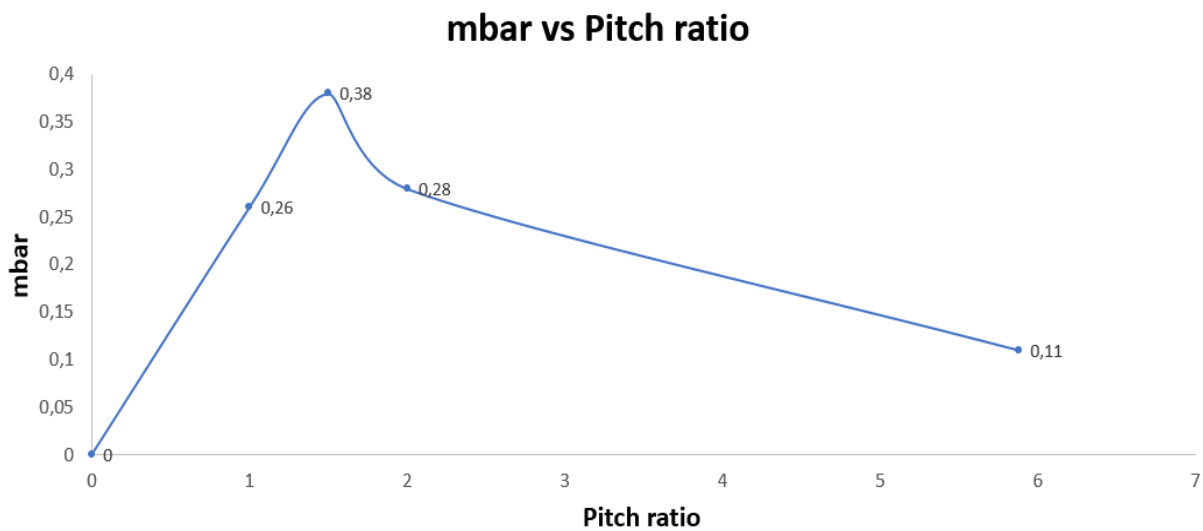


Figure 39: mbar vs pitch ratio for Impeller 1, 4, 5 and 6. Indicates which impeller generates the largest pressure.

The theory presented in Section 4.2.3 states that maximal flow is generated at a pitch ratio equal to 1.5. The screw used by professor Yeng-Yung Tsui in his experiment was a single bladed helix. When used in the well the HydraArchimedes™ tool is exposed to extreme conditions. It is therefore important that the tool can withstand these conditions. Based on these factors and Yeng-Yung Tsui's observations, it was decided to test the optimal pitch ratio for two bladed screw impellers. The graph presented in Figure 39 indicates that also two bladed impellers generate maximum flow at a pitch ratio equal to 1.5 in the well. In order for the cement insurance tool to function more as a restrictor in the well, it is therefore recommended to use an impeller with a pitch ratio equal to 1.5 and having double threaded blades.

6.2 Dye-test

In this section, the displacement effect for the different impeller designs is analyzed and discussed. As in Section 3.2.2, dye was injected into the test-chamber and the displacement effect was shown on the outside of the casing. Section 6.2.1 shows the displacement effect when rotating at 50 RPMs, while Section 6.2.2 shows the displacement effect when rotating at 100 RPMs. Each picture represents a single test with a given impeller design. The number above each picture represents the impeller design tested. For example, (1) means that the picture below represents the results for Impeller 1. Picture 0 in Figure 40 and 41 represents the displacement effect from the HydraArchimedes™ tool. Impellers 4 and 5 were not dye-tested because their geometries were too similar to Impeller 1, and because the graph in Figure 39 indicated that Impeller 1 generated the largest amount of pressure.

6.2.1 Dye-testing at 50 RPM

Figure 40 is a collage of seven pictures and each picture represents an impeller rotated at 50 RPM. As in Chapter 3 these pictures below were obtained by filming with an iPhone 7, and each film was stopped after four seconds, and screenshotted. Each picture shows the manner in which the dye was displaced by the impeller after four seconds of interaction, and the pictures can therefore be fairly compared to each other.

The pictures below clearly indicate a large difference in fluid displacement for the different impeller geometries. These pictures can actually be categorized into three different categories. Category one contains the HydraArchimedes™ tool, Impeller 6 and Impeller 9. These impellers generated the worst dye displacement and left some uncoloured spaces on the outside of the casing. The second category contains Impellers 2, 3 and 7. These impellers generated medium dye displacement, because the colour was evenly distributed, and left few uncoloured spaces. However, the intensity of the colour was poor, indicating that most of the dye was moving up between the impeller and the casing. The third, and final category, contains Impeller 1 and Impeller 8. These two impellers generated evenly distributed dye displacement and a very strong colour intensity as compared to the other impellers. The colour column for Impeller 1 and 8 are also larger compared to the different impellers. It is difficult to differentiate between pictures 1 and 8. If taking a closer look at the two pictures, it can be seen that Impeller 1 generated a slightly stronger colour intensity.

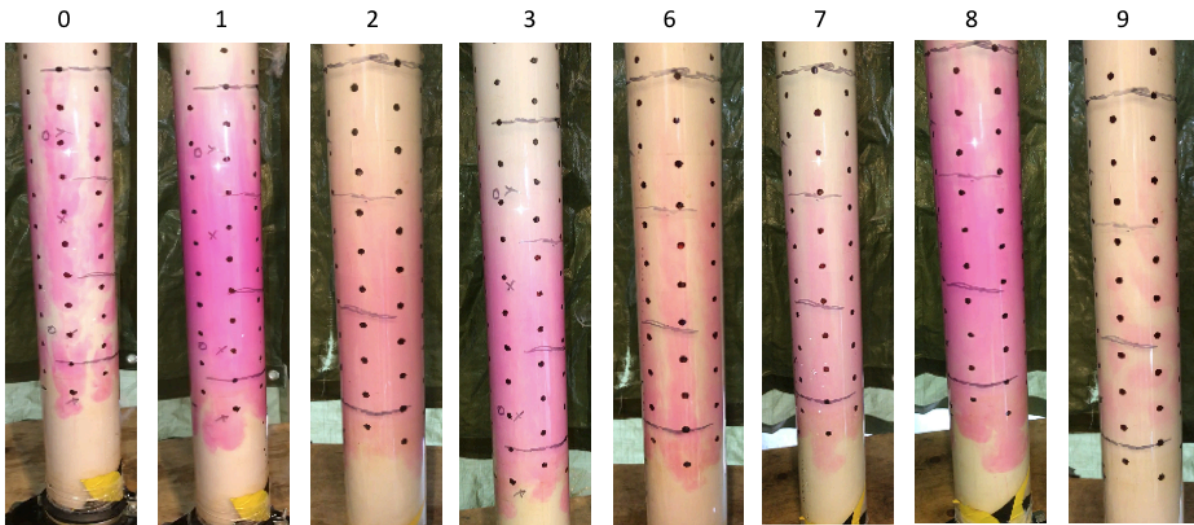


Figure 40: Dye displacement test at 50 RPM. Injecting dye during water circulation and impeller rotation.

6.2.2 Dye-testing at 100 RPM

Similar tests are shown in Figure 41, however the impellers were rotated at 100 RPM. Each film was stopped after three seconds and not four seconds as above, and screenshotted. This is because most of the dye had disappeared after four seconds and therefore could some of the impellers not be used for comparison.

When comparing Figures 40 and 41 it can be seen that the results are very similar, except for Impeller 7 now showing a more evenly distributed and intense colour. This may be due to its higher efficiency at high RPMs, or it may be the results of an error in the dye powder measurement. As in Figure 40, two impellers stood out, namely Impeller 1 and Impeller 8. It can be seen from Pictures 1 and 8 in Figure 41 that the corresponding impellers generated a slightly less intense colour compared to that of the pictures in Figure 40. The reason for this may be the extreme displacement effect of the impellers. When rotating these two impellers at 100 RPM for four seconds, most of the dye was circulated out of the system.

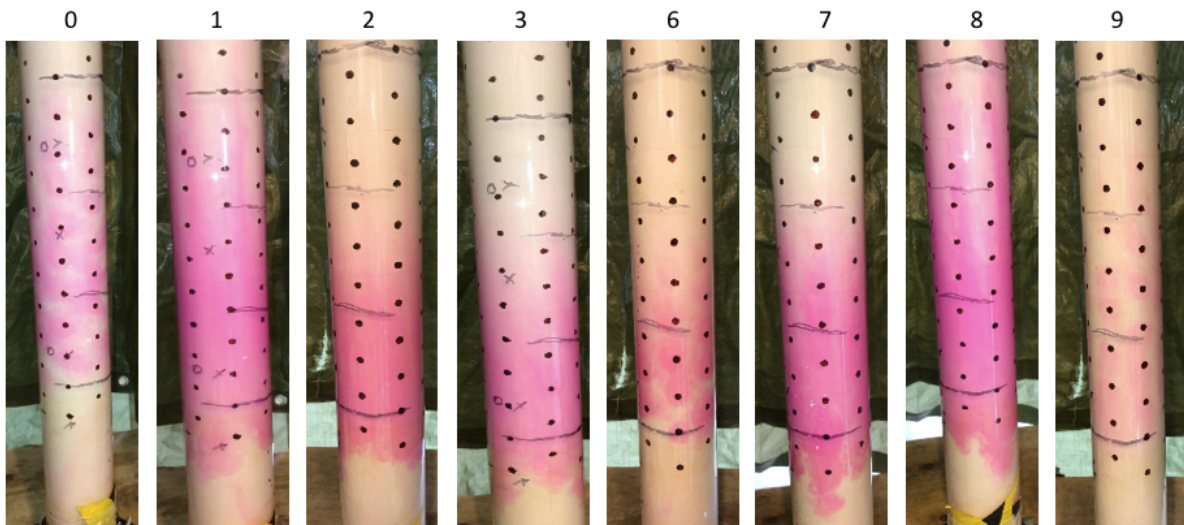


Figure 41: Dye displacement test at 100 RPM. Injecting dye during water circulation and impeller rotation.

As mentioned earlier in this thesis, the most important thing during a P&A operation is to create a proper rock-to-rock barrier in the well. When conducting the operation with PWC[®] instead of milling, it is more challenging to fill the annular space with cement. The pictures in Figures 40 and 41 provide a representation of the manner in which the impellers of Chapter 5 will displace cement on the outside of the casing in full-scale. Pictures 0 in Figure 40 and 41 are the same pictures obtained for the HydraArchimedes[™] tool in Section 3.2.2.1. In Chapter 3, it was concluded that the HydraArchimedes[™] tool could be improved since it did not colour the whole surface area of the casing. The dye displacement results for the HydraArchimedes[™] tool were used in this section for comparison. Based on the dye displacement tests above, the displacement effect of Impeller 1 and Impeller 8 was considerably better than that of the HydraArchimedes[™] tool. Considering the extreme conditions inside a well Impeller 1 is probably the best design. Increasing the number of blades from one to two blades also decreased the damaging vibrations during rotation.

Should the mechanical impact from casing to the HydraArchimedes[™] tool prove too significant, an option could be to decrease the OD of the tool. The tests above indicate that Impeller 2, which had a decreased OD, displaced the dye very efficiently as compared to the HydraArchimedes[™] tool. The colour intensity at 50 RPM was slightly weaker than at 100 RPM. At both 50 and 100 RPM however, Impeller 2 displaced cement over the entire surface area of the casing, which is not the case for the HydraArchimedes[™] tool. Therefore, Impeller 2 seems to be a good alternative to the HydraArchimedes[™] tool.

Axial flow impellers are designed to generate a downward flow, while radial flow impellers are designed to generate an outward radial flow, see Section 4.3. Inside the casing, cement is flowing over the HydraArchimedes™ tool, and the perforations are always 90 degrees from the impeller. Therefore, the idea with the radial flow impeller, Impeller 9, was to push the cement perpendicular out from the impeller, thereby flowing straight out through the perforations and into the surrounding annulus. Picture 9 in Figure 40 and 41 indicates that Impeller 9 generates the worst dye displacement. Based on these observations, Impeller 9 is not preferred for this type of operation.

6.3 Computational fluid dynamics

CFD is a method that uses numerical analysis and data structures to investigate the flow of a fluid, usually through or around an object. Supercomputers are used to solve complex equations and provide efficient and reliable simulations of real case scenarios. Computer simulation reduces the need for costly prototypes and eliminates rework and delays, thereby saving time and development costs.

Based on the findings in Chapter 3, Section 6.1 and Section 6.2, CFD–analyses have been conducted on the cement insurance tool used today, the HydraArchimedes™ tool, and the most promising impeller from Section 6.1 and 6.2, Impeller 1. Since the time was limited, the CFD-analyses were performed by an external company named DEPIAK Industrial Technology Corporation [32]. The analyses and parameters used for this purpose were based on a real well in the North Sea. In the simulation, the well was initially filled with a 14.5 ppg water-based-mud (WBM), which was then displaced with a 16.3 ppg cement. During the operation, the cement pump rate was 138 gpm and the RPM was 120.

Section 6.3.1 presents the results achieved by running the HydraArchimedes™ tool design in the CFD-simulation, while Section 6.3.2 presents the results from running the Impeller 1 design with the exact same parameters.

6.3.1 CFD-analysis HydraArchimedes™

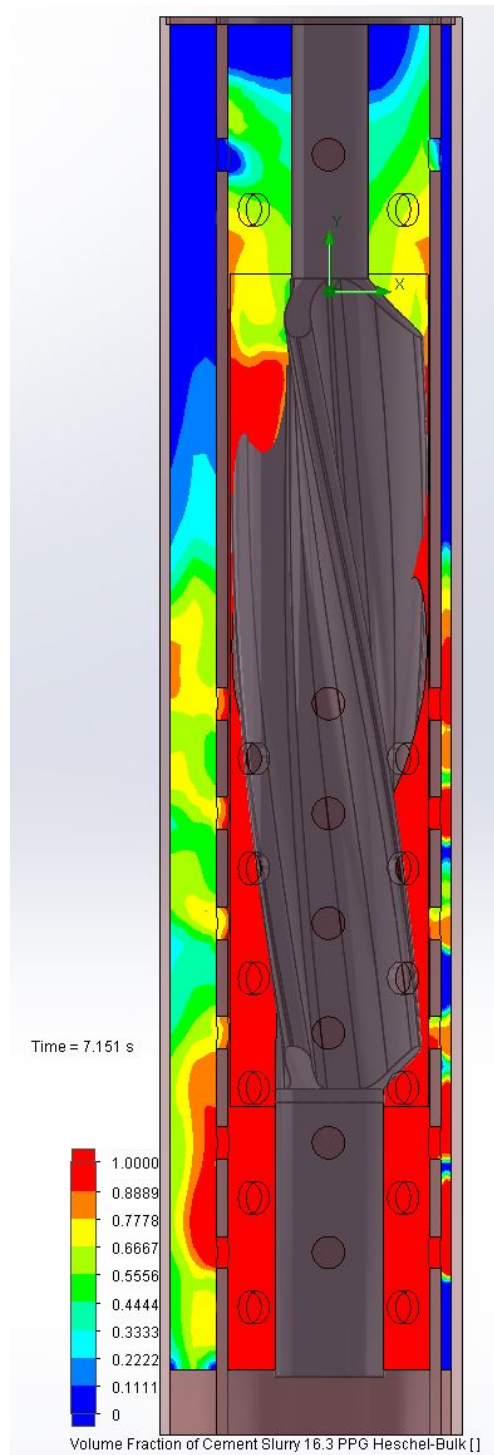


Figure 42: The HydraArchimedes™ cement slurry volume concentration showing displacement of the mud after 7.151 s. Red indicate 100% cement and blue indicate 100% mud [32].

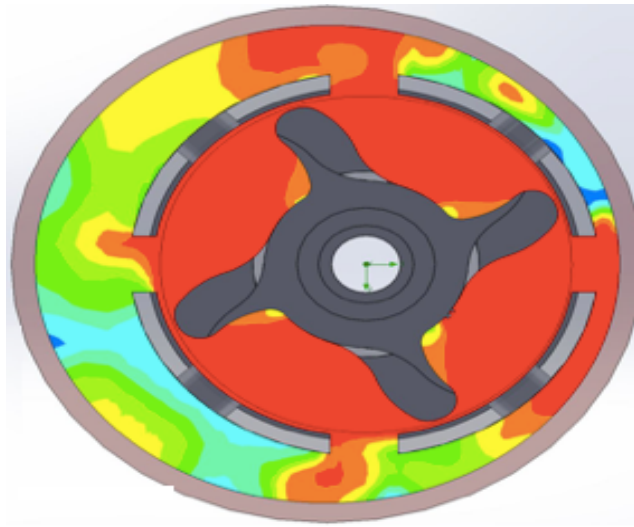


Figure 43: Cement concentration plotted on the cross-section in the perforated casing along the lower part of the HydraArchimedes™ after 7.151 s [32].

Figures 42 and 43 both represent snapshots of an animation showing the manner in which mud was displaced by cement in the casing and in the annular space after 7.51s. Blue indicates 100% mud and red indicates 100% cement. Figure 42 shows that a lot of the mud was displaced by the cement on the outside of the casing. In some places, the mud was displaced 100%, while in other places the mud was displaced only slightly. Figure 42 indicates that, in some small places on the low-side (indicated with blue pockets) the mud was not displaced properly. In Figure 42, much of the cement passed over the HydraArchimedes™ tool inside of the casing, indicating that the HydraArchimedes™ tool was not an optimized restrictor to the cement flow. However, Figures 42 and 43 both show that a lot of the mud was displaced by cement on the outside of the casing. Since the restrictor-effect was lacking the displacement effect had to be due to the wiping action of the tool blades. Figure 43 shows that the wiping action had a good effect on the low-side of the casing. The results of the CFD-analysis confirmed the results obtained from small-scale testing in Chapter 3. Since it was not possible to test the wiping effect in small-scale, the CFD-analysis proved useful to confirm the presence of the wiping action from the rubber blades. The CFD-analysis also confirmed the pressure results obtained in Section 3.2.1.1, which showed that the HydraArchimedes™ tool did not generate a significant downdraft along its axis capable of diverting the fluid flow out through the perforations and into the surrounding annulus.

6.3.2 CFD-analysis Impeller 1

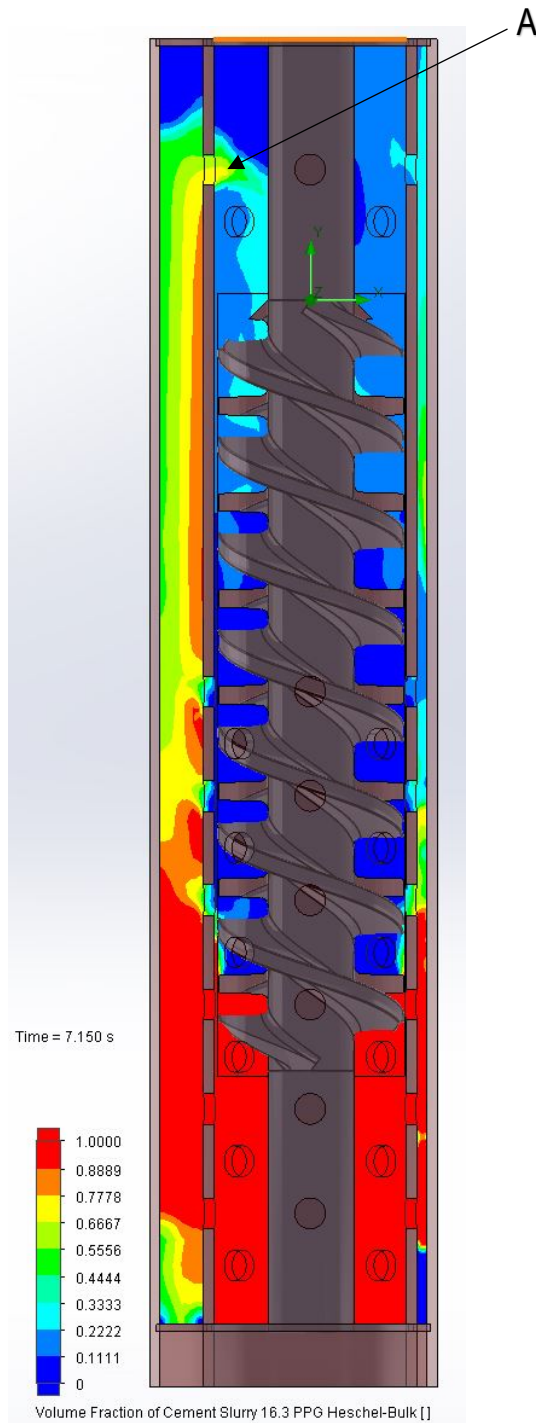


Figure 44: Impeller 1 cement slurry volume concentrations showing displacement of the mud after 7.150 s. Red indicate 100% cement and blue indicate 100% mud [32].

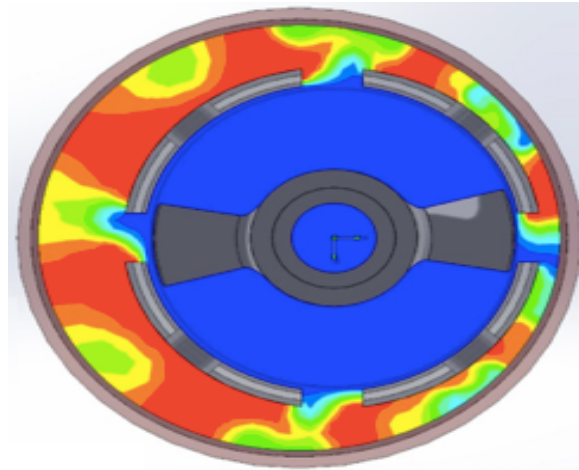


Figure 45: Cement concentration plotted on the cross-section in the perforated casing along the lower part of Impeller 1 after 7.150 s [32].

Similar to Figures 42 and 43, Figures 44 and 45 are snapshots after 7.51s. Figure 44 shows that almost all of the mud was displaced by the cement on the outside of the casing and no clear blue pockets were detected, which indicates very good cement displacement in the annulus. Figure 45 also shows that most of the mud was displaced by cement, indicated by almost no blue colour on the outside of the casing. When comparing Figure 43 and 45, it appears the displacement effect of Impeller 1 is better on the high-side, whereas the displacement effect of the HydraArchimedes™ tool is better on the low-side.

Based on these results and the results obtained in Section 6.1 and 6.2, Impeller 1 appears to generate a more effective restrictor to the cement than that of the HydraArchimedes™ tool. Figure 44 indicates that no mud flowed through and past Impeller 1. Actually, the downdraft it created when rotating Impeller 1 almost seemed to be too good. Point A in Figure 44 shows a strong suction effect on top of Impeller 1. This suction effect will suck the mud present in the annular space into the casing and most likely contaminate the cement being deposited into the annulus. The large pressure generated may also impose unnecessary pressure on the formation and contribute to fluid loss to the formation should there be any obstruction to free flow in the annulus. The results obtained from the CFD-analysis, see Figure 44, were very similar to the results obtained in small scale, see Picture 1 in Figure 41, which indicates very good dye displacement. The suction effect detected on the CFD-analysis also confirmed the strong downward pressure generated by Impeller 1, see Figure 37.

6.3.3 New configuration – Impeller 10 x HydraArchimedes™

Since the small-scale tests and the CFD-analysis indicated that Impeller 1 and the HydraArchimedes™ tool both had certain advantages, it was decided to test a new configuration in which both designs were used, see Figure 46. Because Impeller 1 created a strong downward pressure, this impeller was placed on top of the HydraArchimedes™ tool, which diverts the fluid into the surrounding annulus. In order to reduce any unwanted downdraft, which was discovered in context of Figure 44, Impeller 1 was modified slightly. The OD of the impeller was reduced by 6.35 mm (¼”) and the length of the impeller was reduced by approximately 50 %. This way, cement could pass the impeller and prevent the mud from flowing into the casing, such as in Figure 44. This new impeller is referred to as Impeller 10. See Figure 47. Results from the pressure testing in Section 6.1.2 indicated that by reducing the OD of the impeller by 12.7 mm (½”) (Impeller 2) the pressure generated was reduced by 62 % on average, whereas reducing the length of the impeller (Impeller 3) by 33 % the pressure generated was reduced by 51 % on average. As compared to the efficiency of the HydraArchimedes™ tool these impellers generate 11 and 14 times more pressure, respectively, on average. Thereby allowing these impellers to function as very effective restrictors to cement in a well. Section 6.3.3.1 and 6.3.3.2 contains the results obtained from pressure and dye-testing the new configuration, while Section 6.3.3.3 contains results obtained through the CFD-analysis. The new configuration is referred to as MK2.

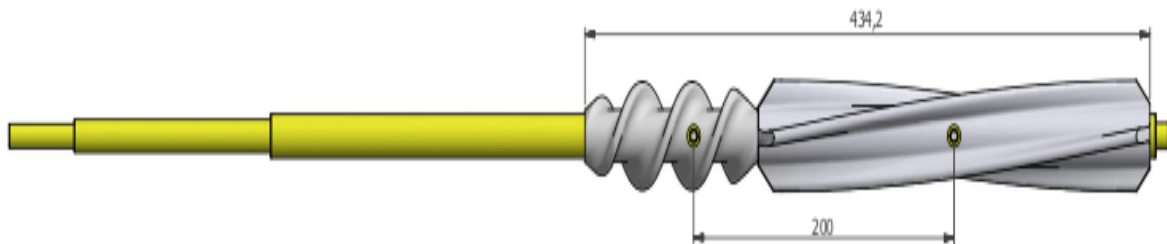


Figure 46: Shaft with the MK2 configuration mounted on.

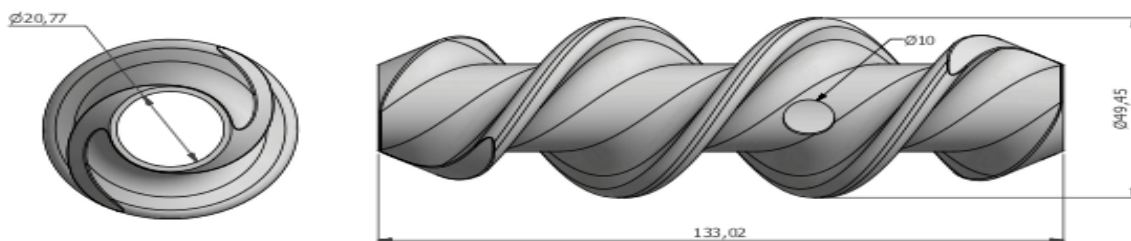


Figure 47: Impeller 10.

6.3.3.1 Pressure-test MK2 configuration

Figure 48 shows a comparison of the pressure generated by Impeller 1, the HydraArchimedes™ tool, Impeller 10 and the MK2 configuration. The test procedure was the same as in Section 3.2.1.1 and in Section 6.1.1. Impeller 1 (blue line) and the HydraArchimedes™ tool (red line) used the same data as in Figure 37. Figure 48 shows that the combined effect of reducing the OD and the length of Impeller 1 (Impeller 10) dramatically reduced the pressure, on average by 57 %. Interestingly Figure 48 shows that the combined effect of Impeller 10 and the HydraArchimedes™ tool (MK2 configuration) actually increased the pressure generated as compared to that of Impeller 10 alone. With the MK2 configuration, the pressure generated was only reduced by 35 % on average, as compared to that of Impeller 1. This implies that the MK2 configuration generated 22 % more pressure on average than Impeller 10. As compared to the HydraArchimedes™ tool, the MK2 configuration generated on average 17 times more pressure, which was a substantial improvement.

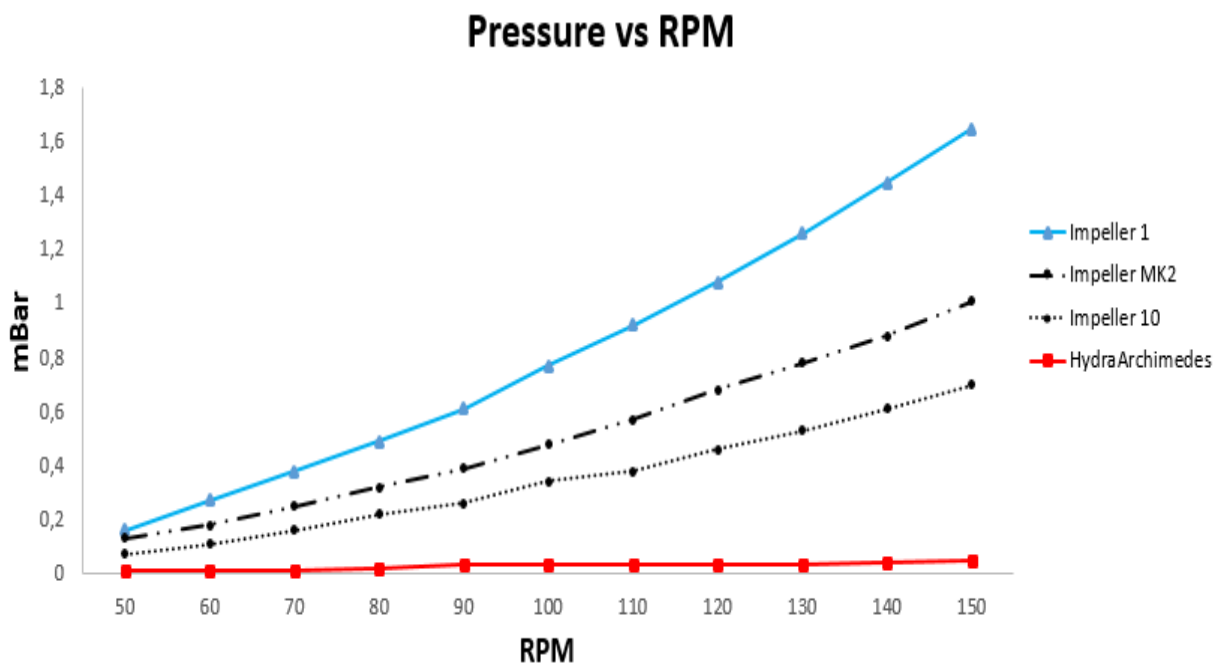


Figure 48: Showing pressure generation vs RPM for four different impeller configurations.

6.3.3.2 Dye-test MK2 configuration

In this section, the dye displacement effect from the HydraArchimedes™ tool and the MK2 configuration was tested and compared. Figures 49 and 50 show the manner in which the two different configurations displaced dye at 50 and 100 RPMs, respectively. The tests were conducted with the exact same parameters as in Section 6.2, $1.2126 * 10^{-4} \frac{m^3}{s}$ (1.92 gpm) and 0.03 g dye. The pictures presented in Figures 49 and 50 represent how the dye was displaced after four seconds. The left picture in Figure 49 and 50 shows dye displacement with the HydraArchimedes™ tool, which was analysed in Section 3.2.2 and which is included in this section for comparison. Figure 49 shows that the MK2 configuration (right picture) displaced dye more efficiently than the HydraArchimedes™ tool at 50 RPM. However, none of these two tools covers the whole surface area purple. Figure 50 shows that both the HydraArchimedes™ tool and the MK2 configuration displaced cement more efficiently at 100 RPMs than at 50 RPMs. The left picture in Figure 50 shows that the HydraArchimedes™ tool covered much of the surface area section purple but left some uncolored spaces between the perforations. The MK2 configuration however, appeared to generate a strong and evenly distributed purple colour across the entire casing surface, indicating a more efficient displacement action.

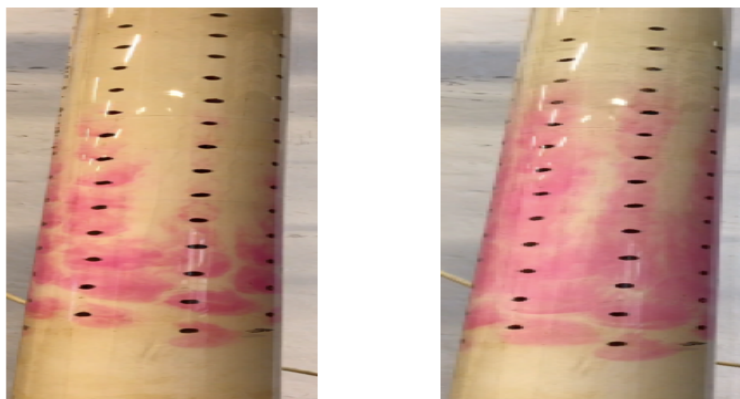


Figure 49: Dye-test at 50 RPM – HydraArchimedes™ (left) and MK2 configuration (right).

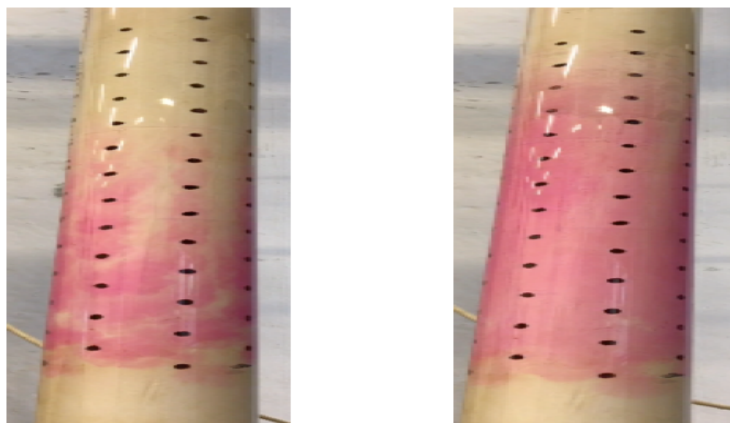


Figure 50: Dye-test at 100 RPM – HydraArchimedes™ (left) and MK2 configuration (right).

6.3.3.3 CFD-analysis MK2 configuration

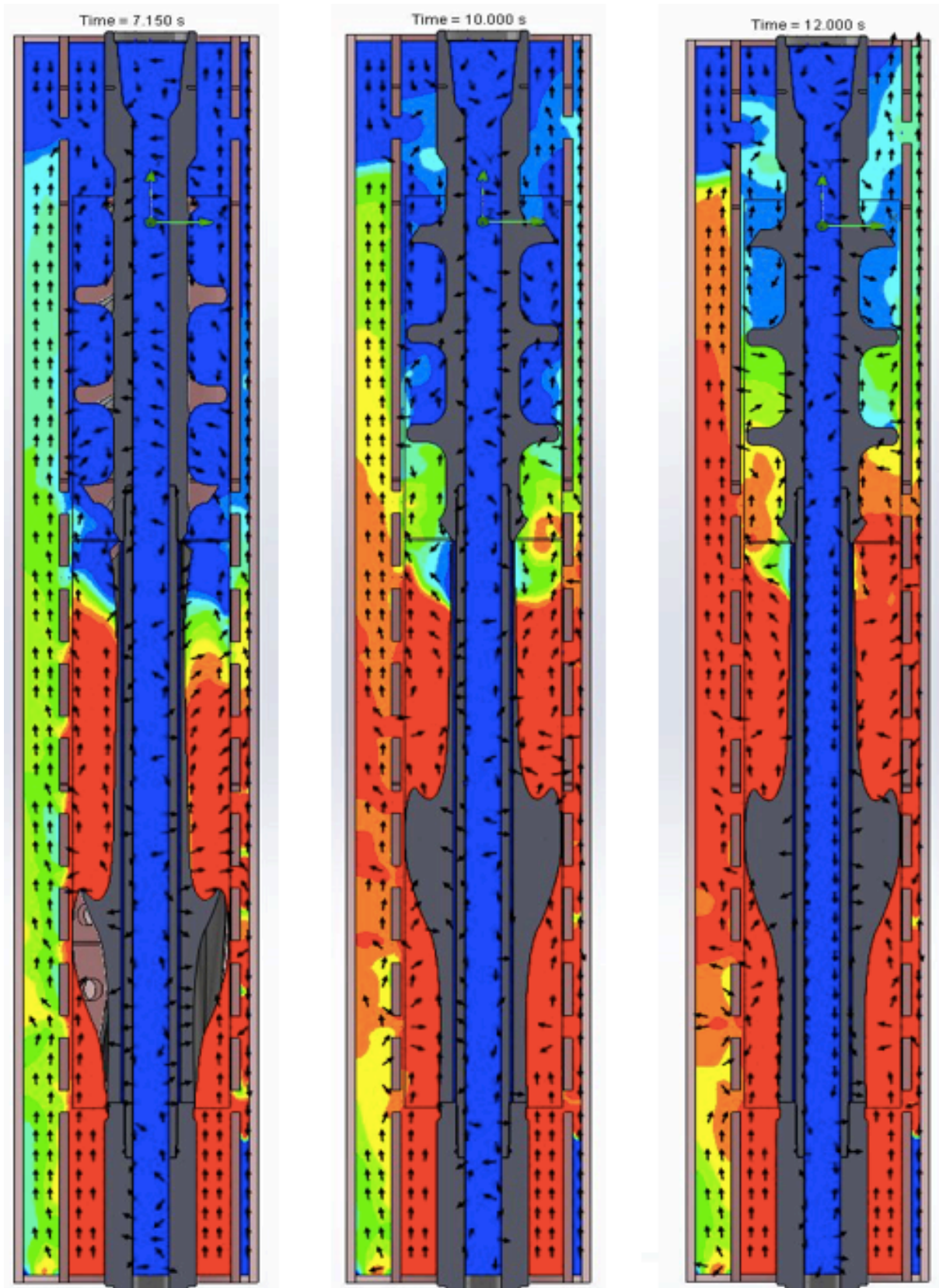


Figure 51: MK2 configuration cement slurry volume concentrations showing displacement of the mud after 7.15 s, 10 s and 12 s, respectively [33].

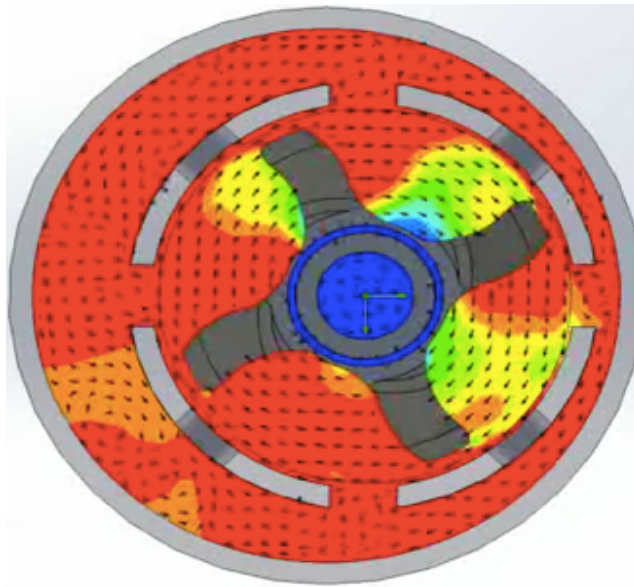


Figure 52: Cement concentration plotted on the cross-section in the perforated casing along the lower part of the MK2 configuration after 12 s [33].

As in Section 6.3.1 and in Section 6.3.2, the left picture in Figure 51 shows the manner in which the cement was displaced after 7.15 s. The CFD-analyses, left picture in Figure 51, confirms the good displacement results obtained from dye-testing the MK2 configuration, see right picture in Figure 50. Figure 51 shows that the MK2 configuration displaced mud very efficiently after 7.15 s, almost 100 %, on the low-side as no blue pockets were detected. On the high-side, however, only 50 % of the mud was displaced after 7.15 s. The middle and right pictures in Figure 51 shows the manner in which the MK2 configuration displaced cement after 10 and 12 s, respectively. It can be seen from these two pictures that the displacement effect gets gradually improved with increasing time. After 12 s, almost 100 % of the mud was displaced by the cement. Figure 52 is a cross-sectional view of the right picture in Figure 51 and shows that the MK2 configuration displaced almost 100 % of the mud after 12 s.

The pictures in Figure 51 also shows that the downdraft discovered in Figure 44 was reduced after reducing the OD and the length of Impeller 1. A close look shows that some cement had moved up between the impeller and the casing, thereby preventing mud from flowing into the casing. However, some notable downdraft appeared to be present. Further testing should therefore be carried out to check if this downdraft causes the mud to contaminate the fresh cement.

7 Conclusion

An essential part of this thesis was to modify the test-rig to allow it to circulate water at a scaled rate. Without this modification, it would have been impossible to obtain realistic analyses with respect to the manner in which different impeller displaced cement on the outside of the casing.

As mentioned in Section 5.1, the cement insurance tool currently used by HydraWell is made out of rubber. Since the 3D-printer could not print rubber, the model had to be printed in plastic and tested with a somewhat rigid and inflexible plastic model. Therefore, only the geometry of the cement insurance tool was analysed in the small-scale testing. However, the tests indicated that the cement insurance configuration had some improvement potential. The pressure generating tests showed that the HydraArchimedes™ tool generated the lowest amount of pressure for any given RPM, which indicated that the HydraArchimedes™ tool was not a preferred restrictor in the well. The dye displacement tests conducted in Section 6.2.1 and 6.2.2 also indicated that the HydraArchimedes™ geometry displaced dye less efficiently than most of the other impellers.

After testing several impellers and discussing the results, Impeller 1 generated the best results. This impeller generated the highest amount of pressure and provided the most efficient displacement of dye on the outside of the casing. The results showed that the impeller that generated the highest amount of pressure, also was the impeller that displaced the dye most efficiently. It can therefore be concluded that this restrictor effect in the well has a large effect on the cement displacement efficiency.

Based on the results obtained during the small-scale testing CFD-analysis were conducted. These analyses confirmed the results from small-scale testing and provided valuable extra information regarding the rubber effect of the HydraArchimedes™ tool and also provided information about the suction effect generated by Impeller 1. The CFD-analyses confirmed that the HydraArchimedes™ rubber blades provided an important wiping effect and also that Impeller 1 generated a somewhat excessive downdraft. The CFD-analyses also indicated that the HydraArchimedes™ tool had a good displacement effect on the low-side of the casing, while Impeller 1 had a good effect on the high-side of the casing. Based on these results the MK2 configuration was developed. In the MK2 configuration, the geometries of the HydraArchimedes™ tool and Impeller 1 were combined in one tool, see Figure 45. Both the small-scale testing and the CFD-analyses indicated large improvements in the cement displacement as compared to that of the original HydraArchimedes™ tool.

Based on the experiments and results obtained in this thesis, the most efficient displacement and largest pressure produced were generated by Impeller 1. Considering, however, that the CFD-analyses showed that Impeller 1 generated a downdraft somewhat excessive, and also that the HydraArchimedes™ tool generated an important wiping effect, it is therefore recommended that HydraWell Intervention employs the MK2 configuration as an optimum cement displacement tool. See Figure 53. If manufacturing Impeller 10 in steel, it will also be possible to reuse the impeller several times and thus reduce costs.

Based on the results obtained in this thesis, HydraWell is planning to use the new MK2 configuration, Figure 53, in July 2018 when conducting a full-scale P&A operation in the North Sea for AkerBP.

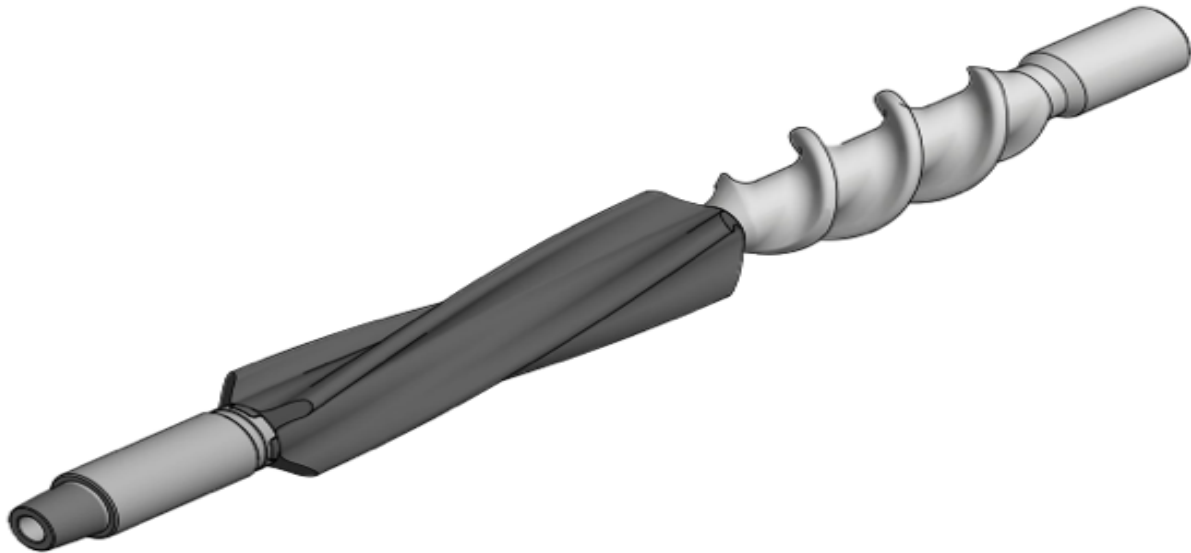


Figure 53: MK2 configuration.

8 Appendix

HydraArchimedes	
Impeller 1	
Impeller 2	
Impeller 3	
Impeller 4	
Impeller 5	
Impeller 6	
Impeller 7	
Impeller 8	
Impeller 9	
Impeller 10	
MK2	

9 References

1. The Norwegian Petroleum Directorate. (2017, 03). Norsk Petroleum. Recieved from <http://www.norskpetroleum.no/en/petroleum-resources/petroleum-formation/>
2. PAF. (2014). Need for new and cost-effective P&A technology. Received from <https://www.norskoljeoggass.no/globalassets/dokumenter/drift/presentasjonerarrangementer/plug--abandonment-seminar-2014/1---need-for-new-and-cost-effective-p-og-a-technology---paf---martin-straume.pdf>
3. NORSOK D-010. (2013). Well Integrity in drilling and well operations. Standard Norge.
4. NORSOK D-010. (2013). Well Integrity in drilling and well operations, p.93. Standard Norge.
5. NORSOK D-010. (2013). Well Integrity in drilling and well operations, p.96. Standard Norge.
6. Weatherford. (2014). Guideline for effective milling.
7. HydraWell. (2015). HydraWell.no. Received from <https://www.hydrawell.no>
8. Steen, C. (2013). P&A operations today and improvement potential .
9. HydraWell . (2017). HydraWell Intervention Handout. Provided by Arne G. Larsen.
10. Rongve & Opaas. (2016). Build and optimize a test rig that can simulate the differential pressure produced by the HydraArchimedes™ during a plug and abandonment operation, as a function of angular velocity.
11. Engineering ToolBox. (2004). Engineeringtoolbox.com. Received from https://www.engineeringtoolbox.com/laminar-transitional-turbulent-flow-d_577.html
12. Engineering. (2016). Engineering Stock Exchange. Received from <https://engineering.stackexchange.com/questions/8004/how-to-calculate-flow-rate-of-water-through-a-pipe>
13. Wikipedia. (2018). Wikipedia.org. Received from <https://en.wikipedia.org/wiki/Propeller>
14. Wikipedia. (2018). Wikipedia.org. Received from <https://en.wikipedia.org/wiki/Archimedes>
15. Wikipedia. (2018). Wikipedia.org. Received from https://no.wikipedia.org/wiki/Arkimedes%27_skrue
16. Quora. (2016). Quora.com. Received from <https://www.quora.com/What-is-the-physical-principle-that-allows-the-Archimedes-Screw-to-work>
17. Wikipedia. (2018). Wikipedia.org. Received from [https://en.wikipedia.org/wiki/Turtle_\(submersible\)](https://en.wikipedia.org/wiki/Turtle_(submersible))

18. History. (2016, 01). History.com. Received from <https://www.history.com/news/history-lists/9-groundbreaking-early-submarines>
19. Marine Insight. (2017, 10). marineinsight.com. Received from <https://www.marineinsight.com/naval-architecture/10-factors-considered-efficient-ship-propeller-design/>
20. P, T. (2017). e-ribbing.com. Received from http://www.e-ribbing.com/index.php?option=com_content&view=article&id=175:propellers-diameter-en&catid=39:propellers&Itemid=256&lang=en
21. Grannies, B. (2013, 08). Evindrudenation.com. Received from <http://www.evinrudenation.com/owner-zone/about-propellers/>
22. Savvyboater. (2014). Savvyboater.com. Received from <http://blog.savvyboater.com/pitch-perfect-selecting-the-right-boat-propeller-pitch/>
23. Rudow, L. (2015). boats.com. Received from http://www.boats.com/how-to/understanding-propeller-pitch/#.WrDZ08gh0_V
24. Wikipedia. (2018). Wikipedia.org. Received from [https://en.wikipedia.org/wiki/Screw_\(simple_machine\)](https://en.wikipedia.org/wiki/Screw_(simple_machine))
25. Tsui, Y.-Y. (2008). Mixing flow characteristics in a vessel agitated by the screw impeller with a draught tube. Taiwan: National Chiao Tung University.
26. Killcaremarina. (2018). killicaremarina.com. Received from <http://www.killicaremarina.com.au/commonly-asked/61-about-propellers>
27. Dynamixinc. (2013). dynamixinc.com. Received from <http://www.dynamixinc.com/mixing-101-the-basic-principles-of-mixing-and-impellers>
28. Smith, J. (2011). thermopedia. Received from <http://www.thermopedia.com/fr/content/549/>
29. Mixerdirect. (2017). Mixerdirect. Received from <http://blog.mixerdirect.com/what-is-the-difference-between-axial-and-radial-flow-impellers>
30. Postmixing. (2013). postmixing.com. Received from <http://www.postmixing.com/mixing%20forum/impellers/impellers.htm>
31. Chemicalonline. (2018). Chemicalonline.com. Received from <https://www.chemicalonline.com/doc/rushton-turbine-0001>
32. Depiak, A and Depiak, K (2018). DEPIAK Industrial Technology Corporation. Handout nr.1 provided by Morten Mhyre
33. Depiak, A and Depiak, K (2018). DEPIAK Industrial Technology Corporation. Handout nr.2 provided by Morten Mhyre